1 **Regular paper**

2 **Fields:** Cell

3

4 **Compounds in cigarette smoke induce EGR1 expression via the AHR, resulting in**

5 **apoptosis and COPD**

6 Naoko Hattori[1, 2, 5, *], Takeya Nakagawa[1, 2, *], Mitsuhiro Yoneda[1, 2, *], Hiromi Hayashida[1, 2], Kaori

7 Nakagawa[1, 2], Kazuo Yamamoto[4], Myo Win Htun[1, 3], Yasuaki Shibata[1, 3], Takehiko Koji[1, 3], and

8 Takashi Ito[1, 2, **]

9

10 [1]Nagasaki University Graduate School of Biomedical Sciences, Nagasaki, Japan

11 [2]Department of Biochemistry, Nagasaki University School of Medicine, Nagasaki, Japan

12 [3]Department of Histology and Cell Biology, Nagasaki University School of Medicine,

13 Nagasaki, Japan

14 [4]Biomedical Research Support Center, Nagasaki University School of Medicine, Nagasaki,

15 Japan

16 [5]Department of Dermatology, Nagasaki University Graduate School of Biomedical Sciences,

17 Nagasaki, Japan.

18 *These authors contributed equally to this manuscript.

19 N.H. initiated and planned this research; T. N. and Y. M. performed a significant number of

20 experiments.

21 **Corresponding author

22 1-12-4 Sakamoto, Nagasaki, Nagasaki 852-8523, Japan TEL: 81-95-819-7037, 7038

23 E-mail: tito@nagasaki-u.ac.jp

24

25   Running title: **CS induces EGR1 expression via the AHR, resulting in apoptosis**

26

27   **Abbreviations:** AHR, aryl hydrocarbon receptor; ANOVA, analysis of variance; ARNT, AHR

28   nuclear translocator; BALF, bronchoalveolar lavage fluid; celiprolol, celiprolol hydrochloride;

29   COPD, chronic obstructive pulmonary disease; CS, cigarette smoke; CYP1A1, cytochrome

30   p450 1A1; DMSO, dimethyl sulfoxide; EGR1, early growth response 1; FICZ, 6-

31   formylindolo[3,2-b] carbazole; HCI, Health Canada Intense; HNB, heat-not-burn; H&E,

32   hematoxylin and eosin; propranolol, propranolol hydrochloride; RPMI, Roswell Park Memorial

33   Institute; NGFI-A, nerve growth factor-induced protein A; NNK, 4-(methylnitrosamino)-1-(3-

34   pyridyl)-1-butanone; NNN, N-nitrosonornicotine; SR1, stemregenin1; TCDD, 2,3,7,8-

35   tetrachlorodibenzo-p-dioxin; TPM, total particulate matter; 5, 6-DMB, 5,6-

36   dimethylbenzimidazole

37 **Abstract**

38   Chronic obstructive pulmonary disease (COPD) is a major cause of mortality

39 worldwide, and pulmonary epithelial cell apoptosis is regarded as one of the most important

40 factors in its pathogenesis. Here we examined the molecular mechanisms of apoptosis caused by

41 cigarette smoke (CS). In the normal bronchial epithelium cell line BEAS-2B, a CS extract

42 markedly induced apoptosis together with transient early growth response 1 (EGR1) protein

43 expression, which is activated over time via the aryl hydrocarbon receptor (AHR). The CS

44 extract induced apoptosis and decreased cell count of BEAS-2B cells and was significantly

45 reversed by knockdown of either *EGR1* or *AHR*. *In vivo*, the CS extract caused alveolar wall

46 destruction, mimicking COPD, 1 week after intrathoracic injection. Bronchoalveolar lavage

47 fluid (BALF) from the CS extract-treated mice contained massive numbers of apoptotic

48 epithelial cells. Furthermore, it was found that aminoanthracene induced EGR1 expression and

49 cell apoptosis. By contrast, the AHR antagonist stemregenin 1 (SR1) restored apoptosis upon

50 CS treatment. These results suggest that aryl hydrocarbons, such as aminoanthracene, induce

51 EGR1 expression via the AHR, resulting in cell apoptosis and that this can be prevented by

52 administration of an antagonist of AHR.

53

54 **Key words: AHR, apoptosis, COPD, cigarette smoke, EGR1**

55

Introduction

COPD is a major cause of mortality worldwide (1). Since it has been reported that COPD contributes to the progression of COVID-19, the treatment of COPD is now in the spotlight (2). COPD is a chronic respiratory disease that is caused by an inflammatory response of the lungs to noxious particles or gasses, resulting in chronic bronchiolitis and emphysema, which causes obstructive airflow (1). Among miscellaneous environmental and genetic risk factors, CS is regarded to be one of the most important in the pathogenesis of COPD (3). Among several mechanisms of COPD pathogenesis, the apoptosis of airway epithelial cells of the lung is regarded as one of the most important. An increase in apoptotic alveolar epithelial and endothelial cells observed in the lungs of COPD patients suggests that apoptosis has a role in the destruction of lung tissue and the development of emphysema and COPD (4).

In order to reduce noxious particles or gasses, tobacco-containing vapor products have been developed worldwide. Heat-not-burn (HNB) products, in which the tobacco is heated without being combusted, have been reported to emit lower levels of harmful compounds than conventional CS (5) (6). CS induces abnormal gene expression, characterized as elevated EGR1 expression, and apoptosis, and the reduction of potentially harmful compounds in HNB products decreased EGR1 responses as well as apoptosis (7).

The *EGR1* gene was first identified as nerve growth factor-induced protein A (*NGFI-A*), and it was subsequently determined that it is an early growth response gene under various forms of stimulation (*8*) (Milbrandt, 1987). *EGR1* expression is regulated by a myriad of secreted molecules and stress factors through numerous regulatory elements located upstream of the *EGR1* coding sequence (*9*) (Havis and Duprez, 2020). This gene was previously identified as a potential novel target of 2,3,7,8-tetrachlorodibenzo-p-dioxin (TCDD) in human lung epithelial cells. EGR1 protein levels were increased by TCDD, which has a high affinity for the AHR (*10*) (Martinez et al., 2004).

4

81   The AHR is a transcription factor that was identified as a TCDD-binding receptor

82   protein that regulates xenobiotic metabolism (*11*) (Murray et al., 2014). The AHR also binds

83   various aryl hydrocarbons, such as indoles, polyphenols, and phenazines, and is involved in the

84   regulation of various biological processes (*12*) (*13*) (*14*) (Bjeldanes et al., 1991) (Amakura et

85   al., 2008) (Moura-Alves et al., 2014). Upon binding of a ligand to the AHR, it translocates from

86   the cytoplasm to the nucleus, dimerizes with AHR nuclear translocator (ARNT), and binds to

87   xenobiotic-responsive elements, resulting in transcriptional activation of target genes (*15*)

88   (Nebert, 2017). The classical target gene encodes for the drug-metabolizing monooxygenase

89   cytochrome P450 1A1 (CYP1A1) (*16*). (Ye et al., 2019).

90   In this report, we determined that CS, but not Ploom TECH or Ploom TECH+ HNB

91   products, induces EGR1 expression via the AHR, resulting in apoptosis *in vitro*. CS, but not

92   Ploom TECH or Ploom TECH+ HNB products, induces apoptosis of epithelial cells in BALF

93   and causes alveolar wall destruction. The representative aryl hydrocarbons 1-aminoanthracene

94   and 2-aminoanthracene were found to induce EGR1 expression and apoptosis. Finally, we

95   identified AHR antagonists that decrease the expression of EGR1 and restore apoptosis by CS

96   exposure.

97

Material and Methods

Smoke and aerosol generation

Smoking extracts were prepared as previously described (5) (Takahashi et al., 2018). Briefly, 3R4F cigarettes were obtained from the Kentucky Tobacco Research and Development Center at the University of Kentucky (Lexington, KY, USA). Two HNB products, Ploom TECH and its flavored version, Ploom TECH+, were obtained from Japan Tobacco Inc. (Tokyo, Japan). Untreated 3R4F CS and aerosols from Ploom TECH or Ploom TECH+ HNB products were generated by machine smoking using Health Canada Intense (HCI) puffing conditions (55 mL puff volume, 2-s duration, 30-s puff interval, and a bell-shaped puff profile). The 3R4F cigarette was smoked until the remaining butt length was 35 mm. For the HNB products, the total puff number for each aerosol collection per tobacco capsule was set at 70, which was based on the product specification. Aerosols were dissolved in dimethyl sulfoxide (DMSO) at a concentration of 40 mg/ml for 3R4F extract and 100 mg/ml for both Ploom TECH and Ploom TECH+ extracts.

Cell culture

BEAS-2B cells were cultured in a humidified chamber (37°C, 5% CO_2 in air) with Roswell Park Memorial Institute (RPMI) medium, and the cells were supplemented with 10 µg/ml gentamicin and 10% fetal calf serum (Life Technologies).

siRNA treatment

To determine cell count, BEAS-2B cells were typically seeded into 24-well plates at a density of 0.4×10^4 cells/well. The cells were then transfected with 12 nM siRNAs using Lipofectamine RNAi MAX reagents (Thermo Fisher Scientific).

For the annexin V–PE assay, BEAS-2B cells were seeded into 6-well plates at a density of 1.0×10^5 cells/well. The cells were then transfected with 14 nM siRNAs using

6

124   Lipofectamine RNAiMAX reagents. After 44 hours, the cells were treated with 0.1% 3R4F

125   extract. After 50 hours, the cells were collected for analysis. To examine whether knockdown

126   of EGR1 was successful, we used 1% 3R4F to induce EGR1 before knockdown (Fig. 3A).

127   The EGR1 expression increased in accordance with the concentration of 3R4F added (Fig.

128   S1G), and the effect of knockdown was unclear using 0.1% 3R4F. For RT-qPCR, BEAS-2B

129   cells were seeded into 6-well plates at a density of 0.6×10^4 cells/well. After 20 hours of

130   incubation, the cells were transfected with 14 nM siRNAs using Lipofectamine RNAiMAX

131   reagents. After 48 hours, the cells were collected for analysis.

132

133   *Western Blotting*

134   BEAS-2B cells were seeded into 6-well plates at a density of 2.0×10^5 cells/well.

135   After 16–20 hours of incubation, the cells were treated with a DMSO or 0.5% 3R4F extract.

136   The cell lysates were prepared using a sodium dodecyl sulfate (SDS) buffer and 2–12 hours

137   later, separated by SDS-PAGE (12%), transferred to a nitrocellulose membrane (Bio-Rad), and

138   blocked with 3% BSA in Tris-buffered saline containing 0.05% Tween-20 (TBST). To detect

139   EGR1, the membranes were incubated with anti-EGR1 antibodies (cat. no. S-25; Santa Cruz

140   Biotechnology, Inc.; Santa Cruz, CA), washed, and incubated with anti-mouse peroxidase (cat.

141   no. 04-18-18; SeraCare Life Sciences, MA), and the subsequent chemiluminescence was

142   obtained using the ChemiDoc Touch MP imaging system (BIO-RAD, CA). To detect histones,

143   the membranes were incubated with anti-core histone antibodies (*17*), followed by washing and

144   subsequent incubation with protein A conjugated with Alexa Fluor™ 647 (Thermo Fisher

145   Scientific, Waltham, MA, cat. no. p21462). Fluorescence signals were captured by employing a

146   Typhoon™_FLA 9000 imager (GE Healthcare) to scan the probed membranes, with the PMT

147   setting set at 1000 V.

148

149

Plasmid vectors and transfection

The pCMV-SPORT6-EGR1 plasmid was obtained from RIKEN BRC (Tokyo, Japan) (*18-21*). (Itoh et al., 2006; Kimura et al., 2006; Ota et al., 2004; Otsuki et al., 2005). Plasmid pCDNA3 was obtained from Invitrogen, MA. BEAS-2B cells were seeded at 0.7×10^6 cells/well into 10-cm dishes. After 16–20 hours of incubation, plasmid mixtures containing 12 µg pCDNA3 and 12 µg pCMV-SPORT6-EGR1 were transfected by Xfect^{TM} Transfection Reagent (Takara Bio company, Shiga, Japan) according to the manufacturer's protocol. After 48 hours, the cells were analyzed by TUNEL assay.

Cell Count

Typically, one day before counting, BEAS-2B cells were seeded at 0.56×10^4 cells/well into 24-well plates. After 20 hours of incubation, the cells were treated with a control solvent (DMSO or MeOH), 0.1% 3R4F extract, or 100 nM to 10 µM compounds, and the day was designated as day 0. From each well, four images were collected on days 0 and 3. The cells were counted within a 1-mm^2 square for each image, the day-3 cell counts were normalized to day-0 cell counts, and the relative count level was calculated. Cells were transfected with siRNAs two days in advance of the day indicated, basically as previously described (*22*).

RT-qPCR

Typically, BEAS-2B cells were seeded at 2.0×10^5 cells/well into 6-well plates. After 20 hours of incubation, the cells were treated with control solvent (DMSO), 0.1% 3R4F extract, or 100 nM to 10 µM compounds. Cells were transfected with siRNAs two days in advance of the day indicated, as previously described. After 1–6 hours, RNA was isolated, and cDNA was generated from 0.3-0.5 µg total RNA in the presence of an oligo(dT) primer (Life Technologies), random hexamers (Takara), and SuperScript™ III Reverse Transcriptase

176 (Invitrogen) or PrimeScript™ Reverse Transcriptase (Takara). Using SYBR green and

177 appropriate master-mix reagents, real-time RT-PCR was performed with a QuantStudio™ 12K

178 Flex Real-Time PCR System (Thermo Fisher Scientific). Target gene expression levels were

179 normalized to *GAPDH* expression, and the relative expression level was calculated by

180 comparing with the DMSO control. The PCR primers used were:

181 *EGR1*

182 (forward) 5`-AGGCGGCGATTTTTGTATGT-3`,

183 (reverse) 5`-GGGCAATAAAGCGCATTCAA-3`;

184 *AHR*

185 (forward) 5`-TTCAGATTATCAACAGCAAC-3`,

186 (reverse) 5`- TGCTGTGGCTCCACTACTAC-3`;

187 *GAPDH*

188 (forward) 5`-GGAGCGAGATCCCTCCAAAAT-3`,

189 (reverse) 5`- GGCTGTTGTCATACTTCTCATG -3`.

190

191 ***TUNEL assay and FACS analysis***

192 BEAS-2B cells were seeded into a 10-cm dish at a density of 1.0×10^6 cells/dish.

193 After 20 hours of incubation, the cells were treated with 0.5% DMSO, Ploom TECH extract,

194 Ploom TECH+ extract, or 3R4F extract. Six or 24 hours after treatment, the cells were subjected

195 to a TUNEL assay according to the manufacturer's instructions (DeadEnd Fluorometric TUNEL

196 System, Promega). The cells were then incubated with anti-EGR1 antibodies (cat. no. S-25;

197 Santa Cruz Biotechnology, Inc.; Santa Cruz, CA), washed, incubated with protein A conjugated

198 with Alexa Fluor™ 647 (cat. no. p21462; Thermo Fisher Scientific, Waltham, MA,), and

199 analyzed using a FACS Canto II flow cytometer (BD Biosciences). Twenty thousand cells were

200 counted, and 10,000 cells were displayed.

201

Annexin V–PE assay and FACS analysis

BEAS-2B cells were seeded into 6-well plates at a density of 2.0 x 10^5 cells/well. After 20 hours of incubation, the cells were treated with 1 µM staurosporine, 0.1–0.3% 3R4F extract, or 100nM-10 µM compounds. Six or 24 hours later, the cells were subjected to an Annexin V-PE assay according to the manufacturer's instructions (Annexin V-PE Apoptosis detection kit, Biovision) and analyzed using a FACS Canto II flow cytometer. Ten thousand cells were counted, and 10,000 cells were displayed in Figs. 1, 6, and S2; 20,000 cells were counted, and 20,000 cells were displayed in Fig. 5. In Fig. 6H, six independent assays for each condition were performed, followed by duplicate flow cytometer detection. Ten thousand cells were counted for each detection.

Forty-four hours after transfection the siRNA-treated cells were treated with 0.1% 3R4F extract. Six hours later, the cells were subjected to an annexin V–PE assay and analyzed using a FACS Canto II flow cytometer. Twelve independent assays for each condition were performed, followed by quadruplicate flow cytometer detection. Ten thousand cells were counted for each detection.

Histological analysis

BALB/c mice were injected with 100 µL of 6% DMSO, 6% Ploom TECH extract, 6% Ploom TECH+ extract, or 6% 3R4F extract into their intrathoracic cavity (n=4 mice per group). Twenty-four hours later, the tracheas from eight mice (n=2 mice per group) were surgically exposed and a 23-G needle inserted. BALF was obtained by intratracheal instillation of 1 ml PBS into the lung. BALF 200-µL aliquots were centrifuged at 300 x g for 10 min. Cells in BALF were stained with annexin V–PE (1 µL/100 µL) and Hoechst stain (1/5000). Cytospin preparations of stained BALF were centrifuged at 700 rpm for 10 min onto glass slides using a Cytospin™ 4 Cytocentrifuge (Thermo Scientific). Glass slides prepared by this technique were observed with an Olympus fluorescence microscope (cat. no. BX53). After observation, the

228 cells were stained with Giemsa stain solution (MUTO PURE CHEMICALS). For quantitative

229 analyses, stained images were taken with the same laser settings, and the fluorescence intensity

230 was quantified using Image J software with the same parameters. The integrated density of three

231 annexin V–PE-stained pictures was used for the statistical analysis, as previously described

232 (*23*).

233   After seven days, 8 mice (n=2 mice per group) were anesthetized and euthanized. The

234 lungs were infiltrated with 4% paraformaldehyde, embedded in paraffin, and stained with

235 hematoxylin and eosin (H&E). For quantitative analysis, an area within 50 randomly selected

236 alveoli in each H&E-stained image was measured and averaged. Four sets of averages for each

237 condition were used for statistical analysis.

238

239 *Statistics*

240   Data are shown as means ± SD. Levels of significance for comparison between

241 samples were determined by one-way analysis of variance (ANOVA), followed by Dunnett's

242 test. P-values of <0.05 were considered statistically significant. Graph-Pad Prism v7 software

243 was used for analysis.

244

245 *Study approval*

246   Animal care and experiment was done in accordance with the Guidelines for Animal

247 Experimentation of Nagasaki University and with approval of the Institutional Animal Care and

248 Use Committee (approval no. 2109061743).

249

250 **Data Availability Statement**

251   The data that support the findings of this study are available in the methods and

252 material of this article.

11

Results

3R4F extract, but not Ploom TECH or Ploom TECH+ extracts, induce activation of the

EGR1 gene and apoptosis of BEAS-2B cells.

We report here that 0.5% of conventional CS 3R4F extract but not the same

concentration of extract from the two HNB products, Ploom TECH and Ploom TECH+, induced

elevated transcription of the *EGR1* gene and cell apoptosis in BEAS-2B cells. To elucidate the

connection between *EGR1* gene expression and cell apoptosis, we analyzed EGR1 expression

with anti-EGR1 antibodies and apoptosis by performing a TUNEL assay, followed by flow

cytometry. The same percentage of (0.5%) DMSO, Ploom TECH extract, Ploom TECH+

extract, or 3R4F extract were applied to BEAS-2B cells to determine whether they cause

apoptosis. Six hours after treatment of BEAS-2B cells with 3R4F, 2.5% became EGR1-positive,

and 77.1% had undergone apoptosis; after 24 hours, the number of EGR1-positive cells

decreased to 0.4%, and 96.4% had undergone apoptosis. There was no change in the proportion

of apoptotic cells or EGR1-positive cells treated with Ploom TECH extract or Ploom TECH+

extract compared with the DMSO control. (Fig. 1A–H)

In addition to the DeadEnd Fluorometric TUNEL assay, we performed an annexin V–PE assay,

which can detect early apoptosis and is considered to be highly sensitive (*24*). The sensitivity to

apoptosis was tested with diluted 3R4F extract, using staurosuporine as a positive control,

which is known to induce apoptosis in cultured cells (*25*). Apoptosis was observed in 100% of

0.1-0.5% 3R4F-treated cells after 6 or 24 hours. (Fig. 1K–P). We plotted EGR1 expression over

time (Fig. 2A). It is an early-response gene (*26*), and its transient peak expression is 2–4 hours

after exposure to 3R4F. Downregulation after the transient peak is probably due to proteasomal

degradation of the expressed EGR1, rather than due to 3R4F instability (*27*). Even if EGR1

plays a role in apoptosis, most cells exposed to 3R4F became EGR1-negative within 24 hours.

Therefore, the EGR1-negative and TUNEL assay-positive population detected via flow

cytometer might be positive for EGR1 expression transiently during the course of the

279   experiment. Therefore, apoptotic cells need not be EGR1-positive all the time over the course of

280   the experiment, even if EGR1 plays a role in this process. The 2.5% positive rate of EGR1

281   expression at 6 hours is low; however, it may be dependent on the strength of the antibody. To

282   further confirm the involvement of EGR1 expression in apoptosis, we introduced CMV

283   promoter-driven EGR1 into BEAS-2B cells. Apoptotic cells detected by TUNEL assay

284   increased from 0.1% to 3.5% by EGR1 overexpression (Fig. 2B, C). Since apoptosis is induced

285   in 9.7% of cells that overexpressed EGR1 ([Q2/Q2+Q4] x 100), it is possible that additional

286   downstream regulators of the AHR are needed or that transient rather than continuous

287   overexpression is important. These results suggest that EGR1 is involved in the apoptosis

288   induced by 3R4F.

289

290   ***3R4F causes apoptosis via EGR1, which is regulated through the AHR.***

291   In order to clarify the molecular mechanisms that connect 3R4F, EGR1, and apoptosis

292   we investigated regulation of the AHR and EGR1 in BEAS-2B cells, since AHR agonists

293   increase EGR1 expression through post-transcriptional mechanisms in human lung epithelial

294   cells (*10*). To examine whether knockdown of EGR1 can be achieved, we used 1% 3R4F to

295   induce EGR1 before knockdown (Fig. 3A). EGR1 expression increased in accordance with the

296   concentration of 3R4F added (supplementary Fig. 1F, G), and the effect of knockdown was

297   unclear following induction with 0.1% 3R4F. We treated BEAS-2B cells with two different

298   siRNAs for both AHR and EGR1 to exclude off-target effects. Expression of the AHR and

299   EGR1 as determined by RT-qPCR confirmed the efficiency of their knockdown. In addition,

300   knockdown of the AHR decreased the expression of EGR1, while the knockdown of EGR1 did

301   not decrease expression of the AHR (Fig. 3A). This result indicates that the AHR is an upstream

302   regulator of EGR1 expression, consistent with a previous report (*10*). Mechanistically, it has

303   been suggested that 3R4F extract activates the AHR and transcriptional upregulation of genes,

304   including EGR1, resulting in apoptosis. The effect of EGR-1 or AHR knockdown on apoptosis

305   was directly examined by annexin V–PE assay. BEAS-2B cells treated with siEGR1-2, siEGR1-

306   3, or siAHR-1 showed a significant decrease in the intensity of annexin V–PE staining

307   compared with siControl, suggesting a diminished apoptotic cell population due to the

308   knockdown of these genes (Fig. 3B). The corresponding histogram is shown in Fig. S1. The

309   effect of EGR-1 or AHR knockdown on the intensity of annexin V–PE staining was significant

310   but not strong. Together with the fact that overexpression of CMV promoter-driven EGR1 in

311   BEAS-2B cells induces apoptosis (Fig. 2B, C), these results suggest that EGR1 is involved in

312   3R4F-induced apoptosis.

313   Moreover, we examined the changes in cell count of BEAS-2B cells with the

314   knockdown of AHR or EGR1, in addition to treatment with 3R4F extract. Changes in cell count

315   on day 3 are influenced by cell death, including apoptosis, and proliferation of the remaining

316   cells (*28-30*). Knockdown of either the AHR or EGR1 in BEAS-2B cells restored cell count on

317   day 3 to a statistically significant degree (Fig. 3C, D). Therefore, we suggest that the 3R4F

318   extract induces apoptosis through the AHR and subsequent EGR1 expression.

319

320   ***3R4F but not Ploom TECH or Ploom TECH+ extracts induce apoptosis in mouse respiratory***

321   ***epithelial cells and thereby destroy alveolar walls.***

322   To investigate whether 3R4F extract also induces apoptosis *in vivo*, 100 μL of

323   6% DMSO, 6% Ploom TECH extract, 6% Ploom TECH+ extract, or 6% 3R4F extract were

324   injected into the thoracic cavity of BALB/c mice, and pulmonary histology was performed (Fig.

325   4A–H). Alveolar cell destruction and air space enlargement were observed only in lungs treated

326   with 3R4F (Fig. 4G, H) and not in lungs treated with other extracts (Fig. 4A–F). Four sets of 50

327   randomly selected alveoli in each condition were measured, and their sizes compared. (Fig.

328   S2A–D). The area was larger in the 3R4F-treated lung than in the other lungs (Fig. 4Y). As an

329   animal model of emphysema, Gross et al. described the first reliable animal model, which was

330   created by injecting the proteinase papain intratracheally in rats (31). However, these models

331 involved a single massive injury incurred by administration of papain, which is unusual in

332 human trachea and might not reflect the pathogenesis of the human disease, which is produced

333 over decades (32). As a more physiological model, animals were exposed to CS in a smoking

334 apparatus. However, this model requires a long period of observation under undefined

335 conditions, as in mainstream or sidestream applications (33). While our model with a single

336 massive injury via concentrated chemicals does not appear to simulate a physiological injury,

337 we could obtain clear results with standardized research-grade cigarettes from the University of

338 Kentucky that are commonly used for research (http://www.ca.uky.edu/refcig/) and with a

339 defined dose of total particulate matter (TPM).

340 Because alveolar cell destruction was completed 1 week after injection of the 3R4F extract, the

341 BALF was examined within 24 hours. In the 3R4F extract-treated BALF, annexin V–PE

342 fluorescence staining-positive clumps of apoptotic alveolar epithelial cells were detected (Fig.

343 4L, P). However, no clumps of alveolar epithelial cells were detected, and no Annexin V-PE

344 fluorescence-stained positive cells were observed in the BALF treated with DMSO, Ploom

345 TECH extract, or Ploom TECH+ extract. (Fig. 4I–K, M–O). Subsequent May Grunwald-

346 Giemsa staining showed the morphology (Fig. 4Q–T), and higher-magnification images are

347 shown (Fig. 4U-X). Annexin V-PE fluorescence-stained positive clumps of cells were identified

348 as alveolar epithelial cells by the presence of cilia (Fig. 4T, X). The integrated density was

349 significantly higher in the BALF of 3R4F-treated lung (Figs. 4Z and S3). This result indicates

350 that 3R4F extract also causes apoptosis of alveolar cells and subsequent destruction of the

351 alveolar wall *in vivo*.

352

353 ***N-Nitrosonornicotine (NNN), 1-aminoanthracene, and 2-aminoanthracene induce activation***

354 ***of the EGR1 gene and apoptosis in BEAS-2B cells***.

355   Representative aromatic hydrocarbons and compounds in common tobacco were

356 examined for their effects on cell proliferation of BEAS-2B cells in order to identify the

15

357   substances that cause apoptosis. (Fig. 5A, B). Most of the compounds did not affect cell count

358   (Fig. 5A); however, NNN, 1-aminoanthracene, and 2-aminoanthracene decreased cell counts

359   significantly, and 1-aminopyrene and 2-aminofluorene also decreased cell counts, although not

360   significantly (Fig. 5B). RT-qPCR was performed to determine whether the expression of EGR1

361   was upregulated when these compounds were added to the cells. All five compounds showed

362   upregulation of EGR1 (Fig. 5C, D). To confirm whether the decrease of cell count was due to

363   apoptosis, we performed an Annexin V-PE assay and found that 1-aminoanthracene and 2-

364   aminoanthracene induced apoptosis of BEAS-2B cells, while apoptosis could not be detected in

365   NNN, 1-aminopyrene, and 2-aminofluorene treated cells (Fig. 5E–L). 2-aminoanthracene-

366   induced apoptosis occurred more strongly than with 1-aminoanthracene; however, the cell count

367   on day 3 after treatment with 1-aminoanthracene was lower than after treatment with 2-

368   aminoanthracene. Because cell counts on day 3 reflect apoptosis and surviving-cell growth, 1-

369   aminoanthracene might affect surviving-cell growth in addition to apoptosis. NNN (10 μM)

370   decreased cell count on day 3, which reflected both cell death from apoptosis and surviving-cell

371   growth, but 10 μM 4-(methylnitrosamino)-1-(3-pyridyl)-1-butanone (NNK) or 10 μM

372   benzo[a]pyrene did not affect cell count. Since 10 μM NNN did not cause apoptosis, as detected

373   by annexin V–PE assay, the decreased cell count on day 3 via 10 μM NNN might be due to cell

374   death that was not annexin V–PE assay-positive or was due to diminished residual cell growth.

375   Based on the previous report, 0.1% 3R4F contains 1.42 nM NNN, 1.36 nM NNK, and 50 pM

376   benzo[a]pyrene. It is known that over 8000 chemicals are included in 3R4F, and it is assumed

377   that NNN, NNK, and benzo[a]pyrene are not major contributors to apoptosis. 1-, 2-

378   aminoanthracene (10 μM) causes apoptosis; however, its concentration is greater than that of

379   individual chemicals, such as NNN, NNK, or benzo[a]pyrene, that are included in 3R4F.

380

381   ***Antihypertensive drugs restored the decreased cell count by 3R4F extract, and***

382   ***celiprolol suppressed EGR1 activation by this extract.***

16

383   Drugs that antagonize the AHR and prevent apoptosis have the potential to contribute to

384   COPD treatment. Therefore, we investigated the effect of available drugs with aromatic

385   hydrocarbon structures on the number of BEAS-2B cells reduced by 0.1% 3R4F extract

386   treatment (Fig. 6A, B). At day 3 after 0.1% 3R4F treatment, most drugs had no effect on cell

387   counts (Fig. 6A); however, antihypertensive drugs including propranolol hydrochloride

388   (propranolol), celiprolol hydrochloride (celiprolol), candesartan, and amlodipine significantly

389   restored cell count, which had been decreased by treatment with 0.1% 3R4F extract (Fig. 6B).

390   RT-qPCR was performed to determine whether the expression of EGR1 was downregulated

391   when these drugs were added to the cells. Celiprolol significantly downregulated EGR1

392   expression, and propranolol showed downregulation of EGR1, although not significantly (Fig.

393   6C). We assume that the drugs restore apoptosis caused by 3R4F, and we performed Annexin V

394   assay. However, no assurance could be obtained that the apoptosis was recovered by these

395   drugs. These antihypertensive drugs are well characterized and widely used for the treatment of

396   hypertension(*34, 35*). It has been suggested that these drugs decrease cell death or protect

397   residual cells, resulting in cell growth. It is noteworthy that well-known antihypertensive drugs

398   might protect alveolar cells from damage by smoking. The detailed mechanism will be

399   elucidated in the future.

400

401   *AHR antagonists suppressed the apoptosis induced by 3R4F extract.*

402   We tested whether an AHR antagonist, such as CH-223191 or SR1 (*36, 37*), inhibits apoptosis

403   of BEAS-2B cells by 3R4F. Treatment with 3R4F (0.1%) caused 79.0% of cells to become

404   apoptotic compared with the control (Fig. 6D, E), and the addition of 1 μM CH-223191 reduced

405   the number of apoptotic cells to 76.2% (Fig. 6F). Similarly, the addition of 1 μM SR1 reduced

406   the number of apoptotic cells to 71.0% (Fig. 6G). Statistically, the addition of 1 μM SR1

407   reduced annexin V–PE median and mean values significantly compared with 0.1% 3R4F

408   treatment (Fig. 6H). This result indicates that the apoptosis caused by 0.1% 3R4F is inhibited by

17

409   the AHR inhibitor SR1. RT-qPCR was performed to determine whether the expression of EGR1

410   was downregulated by AHR inhibitors. The addition of 10 µM SR1 reduced EGR1 expression

411   compared with 0.1% 3R4F (Fig. 6I). These results suggest that 3R4F-mediated apoptosis is

412   inhibited as a result of AHR inhibition and downregulation of EGR1 by SR1.

413

414

415   **Discussion**

416   In this paper we clarified the molecular mechanisms of CS-induced apoptosis. Our

417   findings are consistent with previous observations that 0.5% extracts of conventional CS, 3R4F,

418   but not of the commercially available HNB products, Ploom TECH and Ploom TECH+, induce

419   BEAS-2B cell apoptosis (*7*) and with the additional observation that this phenomenon is

420   accompanied by transient EGR1 protein expression over time. Since EGR1 is considered to be a

421   novel target for AHR agonists in human lung epithelial cells (*10*), we focused on the AHR and

422   confirmed that it is involved in an apoptotic signaling cascade. Furthermore, it is noteworthy

423   that 1-aminoanthracene and 2-aminoanthracene, which are aryl hydrocarbons, may be

424   implicated in CS extract-induced EGR1 expression and cell apoptosis.

425   For *in vivo* models of COPD, the general procedure is that animals are exposed to CS

426   using a smoking apparatus. However, the disadvantages of this procedure are that diverse

427   factors, including whether a mainstream or sidestream configuration is used, different times of

428   exposure, and different types of chambers, make the evaluation and comparison of results

429   difficult (*33, 38*). On the other hand, a simple emphysema mouse model was successfully

430   established by intraperitoneal injection of CS extract (*39*). We established a similar emphysema

431   mouse model by direct intrathoracic injection of 3R4F CS extract. In order to determine the

432   concentration of 3R4F, we injected 100 µl of 3R4F or DMSO diluted with PBS to 1, 2, 4, or 8%

433   directly into the intrathoracic cavity. After a week the lungs were examined by H&E staining.

434   We determined that the concentration range for 3R4F that causes alveolar cell wall destruction

435   is 4–8%. The observation that the 3R4F extract induces apoptosis and destruction of the

436   alveolar wall *in vivo* compared with the control over a short time period has the advantage of

437   avoiding diverse factors that would be a concern with a smoking apparatus.

438   CS is a complex mixture, containing over 8000 chemicals, many of which have been reported as

439   bioactive substances generated during the process of tobacco combustion (*40*). Because we

440   found that the AHR affects apoptosis in BEAS-2B cells, we focused on chemicals that have an

441   aryl hydrocarbon skeleton, including the tobacco-specific nitrosamines NNK and NNN, which

442   are classified as group 1 carcinogens (*5, 41-43*). The aryl hydrocarbons reported in Fig. 5A,

443   including NNK, did not affect cell count. Other tobacco-specific nitrosamines, such as NNK,

444   decreased cell count and elevated EGR1 expression moderately but did not cause cell apoptosis,

445   as detected by annexin V–PE assay. 1-aminopyrene and 2-aminofluorene elevated EGR1

446   expression but did not decrease cell count significantly and did not cause apoptosis. Only 1-

447   aminoanthracene and 2-aminoanthracene decreased cell count, elevated EGR1 expression, and

448   caused cell apoptosis. As shown in Fig. 2C, 9.7% of cells that overexpressed EGR1

449   ([Q2/Q2+Q4] x 100) underwent apoptosis. It has been suggested that EGR1 plays a role in the

450   apoptosis of 10% of the cells overexpressing EGR1. Therefore, additional factors might be

451   required to induce apoptosis in the other 90% of cells. It is assumed that 1-aminoanthracene and

452   2-aminoanthracene satisfy this requirement.

453   In *in vitro* experiments, we tested several drugs having an aryl hydrocarbon skeleton

454   and found that celiprolol restored the cell count depressed by 3R4F and decreased the

455   expression of EGR1. Unfortunately, it was not clear that celiprolol restores apoptosis caused by

456   3R4F. However, SR1, which is a known antagonist of anti-AHR antibodies, decreased

457   apoptotic cells, as detected by annexin V–PE assay.

458   Our *in vitro* and in vivo results have suggested our conclusion that aryl hydrocarbons,

459   which are components of CS, but at lower levels in HNB products, induce EGR1 expression via

460   the AHR, resulting in apoptosis and COPD. We also speculate that COPD can be prevented by

461   administration of AHR inhibitor as summarized in Fig. 7.

462

463

464

475

476   **Conflicts of interest**

477   The authors declare that they have no conflicts of interest for this article.

478 *References*

479 (1) Pauwels, R.A., and Rabe, K.F. (2004) Burden and clinical features of chronic

480 obstructive pulmonary disease (COPD). *Lancet*. **364**, 613-620

481 (2) Zhao, Q., Meng, M., Kumar, R., Wu, Y., Huang, J., Lian, N., Deng, Y., and Lin, S.

482 (2020) The impact of COPD and smoking history on the severity of COVID-19: A

483 systemic review and meta-analysis. *J Med Virol*. **92**, 1915-1921

484 (3) Barnes, P.J. (2000) Chronic obstructive pulmonary disease. *N Engl J Med*. **343**, 269-

485 280

486 (4) Demedts, I.K., Demoor, T., Bracke, K.R., Joos, G.F., and Brusselle, G.G. (2006) Role

487 of apoptosis in the pathogenesis of COPD and pulmonary emphysema. *Respir Res*. **7**,

488 53

489 (5) Takahashi, Y., Kanemaru, Y., Fukushima, T., Eguchi, K., Yoshida, S., Miller-Holt, J.,

490 and Jones, I. (2018) Chemical analysis and in vitro toxicological evaluation of aerosol

491 from a novel tobacco vapor product: A comparison with cigarette smoke. *Regul Toxicol*

492 *Pharmacol*. **92**, 94-103

493 (6) Sakaguchi, C., Kakehi, A., Minami, N., Kikuchi, A., and Futamura, Y. (2014) Exposure

494 evaluation of adult male Japanese smokers switched to a heated cigarette in a controlled

495 clinical setting. *Regul Toxicol Pharmacol*. **69**, 338-347

496 (7) Hattori, N., Nakagawa, T., Yoneda, M., Nakagawa, K., Hayashida, H., and Ito, T.

497 (2020) Cigarette smoke, but not novel tobacco vapor products, causes epigenetic

498 disruption and cell apoptosis. *Biochem Biophys Rep*. **24**, 100865

499 (8) Milbrandt, J. (1987) A nerve growth factor-induced gene encodes a possible

500 transcriptional regulatory factor. *Science*. **238**, 797-799

501 (9) Havis, E., and Duprez, D. (2020) EGR1 Transcription Factor is a Multifaceted

502 Regulator of Matrix Production in Tendons and Other Connective Tissues.

503 *International journal of molecular sciences*. **21**,

504 (10) Martinez, J.M., Baek, S.J., Mays, D.M., Tithof, P.K., Eling, T.E., and Walker, N.J.

505   (2004) EGR1 is a novel target for AhR agonists in human lung epithelial cells. *Toxicol*

506   *Sci*. **82**, 429-435

507 (11) Murray, I.A., Patterson, A.D., and Perdew, G.H. (2014) Aryl hydrocarbon receptor

508   ligands in cancer: friend and foe. *Nat Rev Cancer*. **14**, 801-814

509 (12) Bjeldanes, L.F., Kim, J.Y., Grose, K.R., Bartholomew, J.C., and Bradfield, C.A. (1991)

510   Aromatic hydrocarbon responsiveness-receptor agonists generated from indole-3-

511   carbinol in vitro and in vivo: comparisons with 2,3,7,8-tetrachlorodibenzo-p-dioxin.

512   *Proc Natl Acad Sci U S A*. **88**, 9543-9547

513 (13) Amakura, Y., Tsutsumi, T., Sasaki, K., Nakamura, M., Yoshida, T., and Maitani, T.

514   (2008) Influence of food polyphenols on aryl hydrocarbon receptor-signaling pathway

515   estimated by in vitro bioassay. *Phytochemistry*. **69**, 3117-3130

516 (14) Moura-Alves, P., Fae, K., Houthuys, E., Dorhoi, A., Kreuchwig, A., Furkert, J.,

517   Barison, N., Diehl, A., Munder, A., Constant, P., Skrahina, T., Guhlich-Bornhof, U.,

518   Klemm, M., Koehler, A.B., Bandermann, S., Goosmann, C., Mollenkopf, H.J., Hurwitz,

519   R., Brinkmann, V., Fillatreau, S., Daffe, M., Tummler, B., Kolbe, M., Oschkinat, H.,

520   Krause, G., and Kaufmann, S.H. (2014) AhR sensing of bacterial pigments regulates

521   antibacterial defence. *Nature*. **512**, 387-392

522 (15) Nebert, D.W. (2017) Aryl hydrocarbon receptor (AHR): "pioneer member" of the basic-

523   helix/loop/helix per-Arnt-sim (bHLH/PAS) family of "sensors" of foreign and

524   endogenous signals. *Prog Lipid Res*. **67**, 38-57

525 (16) Ye, W., Chen, R., Chen, X., Huang, B., Lin, R., Xie, X., Chen, J., Jiang, J., Deng, Y.,

526   and Wen, J. (2019) AhR regulates the expression of human cytochrome P450 1A1

527   (CYP1A1) by recruiting Sp1. *FEBS J*. **286**, 4215-4231

528 (17) Aihara, H., Nakagawa, T., Yasui, K., Ohta, T., Hirose, S., Dhomae, N., Takio, K.,

529   Kaneko, M., Takeshima, Y., Muramatsu, M., and Ito, T. (2004) Nucleosomal histone

530   kinase-1 phosphorylates H2A Thr 119 during mitosis in the early Drosophila embryo.

531   *Genes Dev*. **18**, 877-888

532   (18)   Itoh, M., Yasunishi, A., Imamura, K., Kanamori-Katayama, M., Suzuki, H., Suzuki, M.,

533   Carninci, P., Kawai, J., and Hayashizaki, Y. (2006) Constructing ORFeome resources

534   with removable termination codons. *Biotechniques*. **41**, 44, 46, 48 passim

535   (19)   Kimura, K., Wakamatsu, A., Suzuki, Y., Ota, T., Nishikawa, T., Yamashita, R.,

536   Yamamoto, J., Sekine, M., Tsuritani, K., Wakaguri, H., Ishii, S., Sugiyama, T., Saito,

537   K., Isono, Y., Irie, R., Kushida, N., Yoneyama, T., Otsuka, R., Kanda, K., Yokoi, T.,

538   Kondo, H., Wagatsuma, M., Murakawa, K., Ishida, S., Ishibashi, T., Takahashi-Fujii,

539   A., Tanase, T., Nagai, K., Kikuchi, H., Nakai, K., Isogai, T., and Sugano, S. (2006)

540   Diversification of transcriptional modulation: large-scale identification and

541   characterization of putative alternative promoters of human genes. *Genome Res*. **16**, 55-

542   65

543   (20)   Otsuki, T., Ota, T., Nishikawa, T., Hayashi, K., Suzuki, Y., Yamamoto, J., Wakamatsu,

544   A., Kimura, K., Sakamoto, K., Hatano, N., Kawai, Y., Ishii, S., Saito, K., Kojima, S.,

545   Sugiyama, T., Ono, T., Okano, K., Yoshikawa, Y., Aotsuka, S., Sasaki, N., Hattori, A.,

546   Okumura, K., Nagai, K., Sugano, S., and Isogai, T. (2005) Signal sequence and

547   keyword trap in silico for selection of full-length human cDNAs encoding secretion or

548   membrane proteins from oligo-capped cDNA libraries. *DNA Res*. **12**, 117-126

549   (21)   Ota, T., and Suzuki, Y., and Nishikawa, T., and Otsuki, T., and Sugiyama, T., and Irie,

550   R., and Wakamatsu, A., and Hayashi, K., and Sato, H., and Nagai, K., and Kimura, K.,

551   and Makita, H., and Sekine, M., and Obayashi, M., and Nishi, T., and Shibahara, T.,

552   and Tanaka, T., and Ishii, S., and Yamamoto, J., and Saito, K., and Kawai, Y., and

553   Isono, Y., and Nakamura, Y., and Nagahari, K., and Murakami, K., and Yasuda, T., and

554   Iwayanagi, T., and Wagatsuma, M., and Shiratori, A., and Sudo, H., and Hosoiri, T.,

555   and Kaku, Y., and Kodaira, H., and Kondo, H., and Sugawara, M., and Takahashi, M.,

556   and Kanda, K., and Yokoi, T., and Furuya, T., and Kikkawa, E., and Omura, Y., and

557   Abe, K., and Kamihara, K., and Katsuta, N., and Sato, K., and Tanikawa, M., and

558   Yamazaki, M., and Ninomiya, K., and Ishibashi, T., and Yamashita, H., and Murakawa,

559   K., and Fujimori, K., and Tanai, H., and Kimata, M., and Watanabe, M., and Hiraoka,

560   S., and Chiba, Y., and Ishida, S., and Ono, Y., and Takiguchi, S., and Watanabe, S., and

561   Yosida, M., and Hotuta, T., and Kusano, J., and Kanehori, K., and Takahashi-Fujii, A.,

562   and Hara, H., and Tanase, T.O., and Nomura, Y., and Togiya, S., and Komai, F., and

563   Hara, R., and Takeuchi, K., and Arita, M., and Imose, N., and Musashino, K., and

564   Yuuki, H., and Oshima, A., and Sasaki, N., and Aotsuka, S., and Yoshikawa, Y., and

565   Matsunawa, H., and Ichihara, T., and Shiohata, N., and Sano, S., and Moriya, S., and

566   Momiyama, H., and Satoh, N., and Takami, S., and Terashima, Y., and Suzuki, O., and

567   Nakagawa, S., and Senoh, A., and Mizoguchi, H., and Goto, Y., and Shimizu, F., and

568   Wakebe, H., and Hishigaki, H., and Watanabe, T., and Sugiyama, A., and Takemoto,

569   M., and Kawakami, B., and Yamazaki, M., and Watanabe, K., and Kumagai, A., and

570   Itakura, S., and Fukuzumi, Y., and Fujimori, Y., and Komiyama, M., and Tashiro, H.,

571   and Tanigami, A., and Fujiwara, T., and Ono, T., and Yamada, K., and Fujii, Y., and

572   Ozaki, K., and Hirao, M., and Ohmori, Y., and Kawabata, A., and Hikiji, T., and

573   Kobatake, N., and Inagaki, H., and Ikema, Y., and Okamoto, S., and Okitani, R., and

574   Kawakami, T., and Noguchi, S., and Itoh, T., and Shigeta, K., and Senba, T., and

575   Matsumura, K., and Nakajima, Y., and Mizuno, T., and Morinaga, M., and Sasaki, M.,

576   and Togashi, T., and Oyama, M., and Hata, H., and Watanabe, M., and Komatsu, T.,

577   and Mizushima-Sugano, J., and Satoh, T., and Shirai, Y., and Takahashi, Y., and

578   Nakagawa, K., and Okumura, K., and Nagase, T., and Nomura, N., and Kikuchi, H.,

579   and Masuho, Y., and Yamashita, R., and Nakai, K., and Yada, T., and Nakamura, Y.,

580   and Ohara, O., and Isogai, T., and Sugano, S. (2004) Complete sequencing and

581   characterization of 21,243 full-length human cDNAs. *Nat Genet.* **36**, 40-45

582   (22) Aihara, H., Nakagawa, T., Mizusaki, H., Yoneda, M., Kato, M., Doiguchi, M.,

583   Imamura, Y., Higashi, M., Ikura, T., Hayashi, T., Kodama, Y., Oki, M., Nakayama, T.,

584   Cheung, E., Aburatani, H., Takayama, K.I., Koseki, H., Inoue, S., Takeshima, Y., and

585   Ito, T. (2016) Histone H2A T120 Phosphorylation Promotes Oncogenic Transformation

586   via Upregulation of Cyclin D1. *Mol Cell*. **64**, 176-188

587   (23) Ichise, M., Sakoori, K., Katayama, K.I., Morimura, N., Yamada, K., Ozawa, H.,

588   Matsunaga, H., Hatayama, M., and Aruga, J. (2022) Leucine-Rich Repeats and

589   Transmembrane Domain 2 Controls Protein Sorting in the Striatal Projection System

590   and Its Deficiency Causes Disturbances in Motor Responses and Monoamine

591   Dynamics. *Frontiers in molecular neuroscience*. **15**, 856315

592   (24) Godard, T., Deslandes, E., Lebailly, P., Vigreux, C., Sichel, F., Poul, J.M., and

593   Gauduchon, P. (1999) Early detection of staurosporine-induced apoptosis by comet and

594   annexin V assays. *Histochem Cell Biol*. **112**, 155-161

595   (25) Chae, H.J., Kang, J.S., Byun, J.O., Han, K.S., Kim, D.U., Oh, S.M., Kim, H.M., Chae,

596   S.W., and Kim, H.R. (2000) Molecular mechanism of staurosporine-induced apoptosis

597   in osteoblasts. *Pharmacol Res*. **42**, 373-381

598   (26) Lau, L.F., and Nathans, D. (1987) Expression of a set of growth-related immediate early

599   genes in BALB/c 3T3 cells: coordinate regulation with c-fos or c-myc. *Proc Natl Acad*

600   *Sci U S A*. **84**, 1182-1186

601   (27) Bae, M.H., Jeong, C.H., Kim, S.H., Bae, M.K., Jeong, J.W., Ahn, M.Y., Bae, S.K.,

602   Kim, N.D., Kim, C.W., Kim, K.R., and Kim, K.W. (2002) Regulation of Egr-1 by

603   association with the proteasome component C8. *Biochim Biophys Acta*. **1592**, 163-167

604   (28) Evan, G.I., Brown, L., Whyte, M., and Harrington, E. (1995) Apoptosis and the cell

605   cycle. *Curr Opin Cell Biol*. **7**, 825-834

606   (29) Meikrantz, W., and Schlegel, R. (1995) Apoptosis and the cell cycle. *J Cell Biochem*.

607   **58**, 160-174

608 (30) O'Connor, L., Huang, D.C., O'Reilly, L.A., and Strasser, A. (2000) Apoptosis and cell

609   division. *Curr Opin Cell Biol*. **12**, 257-263

610 (31) Gross, P., Pfitzer, E.A., Tolker, E., Babyak, M.A., and Kaschak, M. (1965)

611   Experimental Emphysema: Its Production with Papain in Normal and Silicotic Rats.

612   *Arch Environ Health*. **11**, 50-58

613 (32) Campbell, E.J. (2000) Animal models of emphysema: the next generations. *J Clin*

614   *Invest*. **106**, 1445-1446

615 (33) Leberl, M., Kratzer, A., and Taraseviciene-Stewart, L. (2013) Tobacco smoke induced

616   COPD/emphysema in the animal model-are we all on the same page? *Front Physiol*. **4**,

617   91

618 (34) Williams, B., Mancia, G., Spiering, W., Agabiti Rosei, E., Azizi, M., Burnier, M.,

619   Clement, D.L., Coca, A., de Simone, G., Dominiczak, A., Kahan, T., Mahfoud, F.,

620   Redon, J., Ruilope, L., Zanchetti, A., Kerins, M., Kjeldsen, S.E., Kreutz, R., Laurent,

621   S., Lip, G.Y.H., McManus, R., Narkiewicz, K., Ruschitzka, F., Schmieder, R.E.,

622   Shlyakhto, E., Tsioufis, C., Aboyans, V., Desormais, I., and Group, E.S.C.S.D. (2018)

623   2018 ESC/ESH Guidelines for the management of arterial hypertension. *Eur Heart J*.

624   **39**, 3021-3104

625 (35) Whelton, P.K., Carey, R.M., Aronow, W.S., Casey, D.E., Jr., Collins, K.J., Dennison

626   Himmelfarb, C., DePalma, S.M., Gidding, S., Jamerson, K.A., Jones, D.W.,

627   MacLaughlin, E.J., Muntner, P., Ovbiagele, B., Smith, S.C., Jr., Spencer, C.C., Stafford,

628   R.S., Taler, S.J., Thomas, R.J., Williams, K.A., Sr., Williamson, J.D., and Wright, J.T.,

629   Jr. (2018) 2017 ACC/AHA/AAPA/ABC/ACPM/AGS/APhA/ASH/ASPC/NMA/PCNA

630   Guideline for the Prevention, Detection, Evaluation, and Management of High Blood

631   Pressure in Adults: Executive Summary: A Report of the American College of

632   Cardiology/American Heart Association Task Force on Clinical Practice Guidelines.

633   *Hypertension*. **71**, 1269-1324

634   (36)   Kim, S.H., Henry, E.C., Kim, D.K., Kim, Y.H., Shin, K.J., Han, M.S., Lee, T.G., Kang,

635   J.K., Gasiewicz, T.A., Ryu, S.H., and Suh, P.G. (2006) Novel compound 2-methyl-2H-

636   pyrazole-3-carboxylic acid (2-methyl-4-o-tolylazo-phenyl)-amide (CH-223191)

637   prevents 2,3,7,8-TCDD-induced toxicity by antagonizing the aryl hydrocarbon receptor.

638   *Mol Pharmacol.* **69**, 1871-1878

639   (37)   Boitano, A.E., Wang, J., Romeo, R., Bouchez, L.C., Parker, A.E., Sutton, S.E., Walker,

640   J.R., Flaveny, C.A., Perdew, G.H., Denison, M.S., Schultz, P.G., and Cooke, M.P.

641   (2010) Aryl hydrocarbon receptor antagonists promote the expansion of human

642   hematopoietic stem cells. *Science.* **329**, 1345-1348

643   (38)   Tanner, L., and Single, A.B. (2020) Animal Models Reflecting Chronic Obstructive

644   Pulmonary Disease and Related Respiratory Disorders: Translating Pre-Clinical Data

645   into Clinical Relevance. *J Innate Immun.* **12**, 203-225

646   (39)   Chen, L., Luo, L., Kang, N., He, X., Li, T., and Chen, Y. (2020) The Protective Effect

647   of HBO1 on Cigarette Smoke Extract-Induced Apoptosis in Airway Epithelial Cells. *Int*

648   *J Chron Obstruct Pulmon Dis.* **15**, 15-24

649   (40)   Rodgman, A., and Perfetti, T.A. (2013) *The Chemical Components of Tobacco and*

650   *Tobacco Smoke*, CRC Press,

651   (41)   Gunduz, I., Kondylis, A., Jaccard, G., Renaud, J.M., Hofer, R., Ruffieux, L., and

652   Gadani, F. (2016) Tobacco-specific N-nitrosamines NNN and NNK levels in cigarette

653   brands between 2000 and 2014. *Regul Toxicol Pharmacol.* **76**, 113-120

654   (42)   Hoffmann, D., and Hoffmann, I. (1998) Tobacco smoke components. *Beiträge zur*

655   *Tabakforschung International.* **18**, 49-52

656   (43)   Humans, I.W.G.o.t.E.o.C.R.t. (2007) Smokeless tobacco and some tobacco-specific N-

657   nitrosamines. *IARC Monogr Eval Carcinog Risks Hum.* **89**, 1-592

658   (44)   Safe, S., Lee, S.O., and Jin, U.H. (2013) Role of the aryl hydrocarbon receptor in

659   carcinogenesis and potential as a drug target. *Toxicol Sci.* **135**, 1-16

660   (45)   Mulero-Navarro, S., and Fernandez-Salguero, P.M. (2016) New Trends in Aryl

661   Hydrocarbon Receptor Biology. *Front Cell Dev Biol*. **4**, 45

662

663

664

665   *Table 1. Chemical compounds used in experiments summarized in Figure 4.*

666

667   *Table 2. Drugs used in the experiments summarized in Figure 5.*

668

669   **Figure legends**

670   *Figure 1. 3R4F extract, but not Ploom TECH or Ploom TECH+ extracts, increased EGR1*

671   *expression by 6 hours and induced cell apoptosis over time.*

672   (A–H) BEAS-2B cells were treated with 0.5% DMSO (A, B), 0.5% Ploom TECH

673   extract (C, D), 0.5% Ploom TECH+ extract (E, F), or 0.5% 3R4F extract (G, H). After 6 or 24

674   hours, the cells were analyzed by flow cytometer. Y-axis, TUNEL assay using FITC; X-axis,

675   detection with anti-EGR1 antibody and anti-mouse antibody labeled with Alexa Fluor™ 647.

676   (I–P) BEAS-2B cells were treated with 1 µM staurosporine (J), 0.5% 3R4F extract (K,

677   L), 0.3% 3R4F extract (M, N), 0.1% 3R4F extract (O, P), or untreated (I). After 6 or 24 hours,

678   cells were analyzed by an annexin V–PE assay and by flow cytometer.

679   PT, Ploom Tech; PT+, Ploom Tech+.

680

681   *Figure 2. 3R4F induces an early EGR1 response.*

682   (A) BEAS-2B cells treated with 0.5% DMSO or 0.5% 3R4F were analyzed by western

683   blotting for EGR1 and histones at the time points indicated. Both long and short exposure

684   conditions are shown for EGR1.

685   (B, C) pCDNA3 (B), or pCMV-SPORT6-EGR1 (C) were transfected into BEAS-2B

686   cells. After 48 hours, the cells were subjected to flow cytometer analysis. Y-axis, TUNEL assay

687   using FITC; X-axis, detection with anti-EGR1 antibody and anti-mouse antibody labeled with

688   Alexa Fluor™ 647.

689

690   *Figure 3. 3R4F induces apoptosis through AHR regulation of EGR1.*

691   (A) Knockdown of *EGR1* and *AHR,* using two different siRNAs for each gene, was

692   performed using BEAS-2B cells. After 24 hours, 1% 3R4F extract was added and incubated for

693   another 24 hours. Forty-eight hours after knockdown, cell extracts were analyzed by RT-qPCR.

694   Target gene expression levels were normalized to *GAPDH* expression.

695   (B) Knockdown of *EGR1* and *AHR* using two different siRNAs for each gene was

696   performed using BEAS-2B cells. After 24 hours, 0.1% 3R4F extract was added and incubated

697   for another 24 hours. Forty-eight hours after knockdown, the cells were analyzed using a flow

698   cytometer after performing an annexin V–PE assay. The annexin V–PE mean and median

699   fluorescence intensities are shown.

700   (C) Knockdown of *EGR1* and *AHR* using two different siRNAs for each gene was

701   performed using BEAS-2B cells, as indicated. After 48 hours, 0.1% DMSO or 0.1% 3R4F

702   extract was added, and that time point was designated as day 0. The cells were counted on day

703   0 and day 3.

704   (D)The relative increase in cell count was calculated by dividing the number of cells

705   on day 3 by the number of cells on day 0.

706   (B, D) One-way ANOVA, followed by Dunnett's test. $*P<0.05$, $**P<0.01$,

707   $****P<0.0001$.

708

709 ***Figure 4. 3R4F extract induces destruction of the alveolar wall and apoptosis of alveolar***

710 ***epithelial cells in BALF.***

711   (A–H) H&E staining of 6% DMSO (A, B), 6% Ploom TECH extract (C, D), 6%

712   Ploom TECH+ extract (E, F), or 6% 3R4F extract (G, H) injected mice lung.

713   (I–X) Cells in BALF of 6% DMSO (I, M, Q, U), 6% Ploom TECH extract (J, N, R,

714   V), 6% Ploom TECH+ extract (K, O, S, W), or 6% 3R4F extract (L, P, T, X) injected mice were

715   stained with Hoechst (I–L) and Annexin V-PE (M–P) stains. After fluorescence observation, the

716   cells were stained with May Grunwald-Giemsa (Q–X). The small rectangles within Q, R, S, and

717 T are enlarged and shown in U, V, W, and X, respectively. Scale bars, 50 μm (A–T), 10 μm (U–

718 X). Scale bars, 50 μm (H, P, T), 10 μm (X). (Y) The areas of 50 randomly selected alveoli were

719 calculated using ImageJ software. The images used for analysis are shown in Fig. S3A–D. (Z)

720 The integrated density was calculated using ImageJ software. The images used for analysis are

721 shown in Fig. S4A–P in addition to I–P. **P<0.01, ****P<0.0001.

722

723 *Figure 5. 1-aminoanthracene and 2-aminoanthracene, both of which may be components of*

724 *the 3R4F extract, induce apoptosis in BEAS-2B cells.*

725 (A, B) Compound (10 μM) or the same volume of control (MeOH or DMSO) was

726 added to BEAS-2B cells (day 0). For each well, cells were counted on days 0 and 3, and the

727 relative cell count ~~growth~~ was calculated by dividing the number of cells on day 3 by the

728 number of cells on day 0.

729 (C, D) Compound (10 μM) or the same volume of control (MeOH or DMSO) was

730 added as indicated. After one hour, the cell extracts were analyzed by RT-qPCR. Target gene

731 expression levels were normalized to *GAPDH* expression.

732 (E–L) BEAS-2B cells were plated at a concentration of 2.0 x 10^5 cells/well in 6-well

733 plates. On the next day, BEAS-2B cells were untreated (E) or treated with 0.1% DMSO (F),

734 0.1% 3R4F extract (G), or 10 μM compound (H–L). After 24 hours, the cells were analyzed

735 using the annexin V–PE assay and then by flow cytometer.

736 Control*, MeOH; Control**, DMSO. (A–C) One-way ANOVA followed by

737 Dunnett's test. *P<0.05, **P<0.01, ***P<0.001, ****P<0.0001.

738 NNN, *N*-nitrosonornicotine; NNK, 4-(methylnitrosamino)-1-(3-pyridyl)-1-butanone.

739

740 *Figure 6. The AHR antagonist SR1 inhibits apoptosis induced by 3R4F extract in BEAS-2B*

741 *cells.*

742   (A, B) 3R4F (0.1%) and 100 nM compound or the same volume of control (DMSO)

743   were added to each well (on day 0) as indicated. For each well, the cells were counted on

744   days 0 and 3, and the relative cell count was calculated by dividing the number of cells on day

745   3 by the number of cells on day 0.

746   (C) 3R4F (0.1%) and 100 nM compounds or the same volume of control (DMSO)

747   were added to BEAS-2B cells, as indicated. One hour later, cell extracts were analyzed by RT-

748   qPCR. *EGR1* expression levels were normalized to *GAPDH* expression.

749   (D–G) BEAS–2B cells were treated with 0.1% DMSO (D), 0.1% 3R4F extract (E),

750   0.1% 3R4F extract and 1 μM CH-223191 (F), or 0.1% 3R4F extract and 1 μM SR1 (G), and

751   24 h later, an annexin V–PE assay was performed and analyzed by flow cytometer. The mean

752   and median annexin V–PE values shown in E, F, and G are plotted in H.

753   (I) 3R4F (0.1%), 1 μM CH-223191, or 1 μM SR1 was added to BEAS-2B cells, as

754   indicated. One hour later, cell extracts were analyzed by RT-qPCR. *EGR1* expression levels

755   were normalized to *GAPDH* expression.

756   Control**, DMSO.

757   (A–C) One-way analysis of variance (ANOVA), followed by Dunnett's test.

758   **$P<0.01$, ***$P<0.001$, ****$P<0.0001$.

759   FICZ, 6-formylindolo[3,2-b] carbazole; 5, 6-DMB, 5,6-dimethylbenzimidazole; propranolol,

760   propranolol hydrochloride; celiprolol, celiprolol hydrochloride.

761

762   ***Figure 7. Aryl hydrocarbons contained in CS induce EGR1 expression via the AHR,***

763   ***resulting in apoptosis and COPD.***

764   Aryl hydrocarbons, which are components of CS but present at lower levels in HNB products,

765   bind to the AHR, possibly forming a heterodimer with the AHR nuclear translocator (ARNT)

766   (*11, 44, 45*), resulting in response-element binding and EGR1 expression. EGR1 expression

34

767   plays a role in apoptosis and subsequent COPD. This pathway can be blocked by AHR

768   blockers, such as SR1.

769

770   ***Supplementary Figure 1. Aryl hydrocarbons contained in CS induce EGR1 expression via the***

771   ***AHR, resulting in apoptosis and COPD.***

772   (A–E) Knockdown of EGR1 and AHR using two different siRNAs for each

773   gene was performed using BEAS-2B cells, as indicated. After 24 hours, 0.1% 3R4F extract

774   was added and incubated for another 24 hours. Forty-eight hours after knockdown, the cells

775   were analyzed using a flow cytometer after performing an annexin V–PE assay. The black

776   line indicates 1×10^4, and the blue line indicates the median. (F) 3R4F (0.1–0.5%) or the same

777   volume of control (DMSO) was added to each well (on day 0), as indicated. The cells were

778   counted on days 0 and 3, and the relative cell count was calculated by dividing the number of

779   cells on day 3 by the number of cells on day 0. (G) 3R4F (0.1–0.5%) or the same volume of

780   control (DMSO) was added to BEAS-2B cells, as indicated. After one hour, the cell extracts

781   were analyzed by RT-qPCR. *EGR1* expression levels were normalized to *GAPDH* expression.

782

783   ***Supplementary Figure 2.*** *The images used for analysis* ***in Figure 4Y.***

784

785   ***Supplementary Figure 3.*** *The images used for analysis* ***in Figure 4Z.***

786

Graphical Abstract
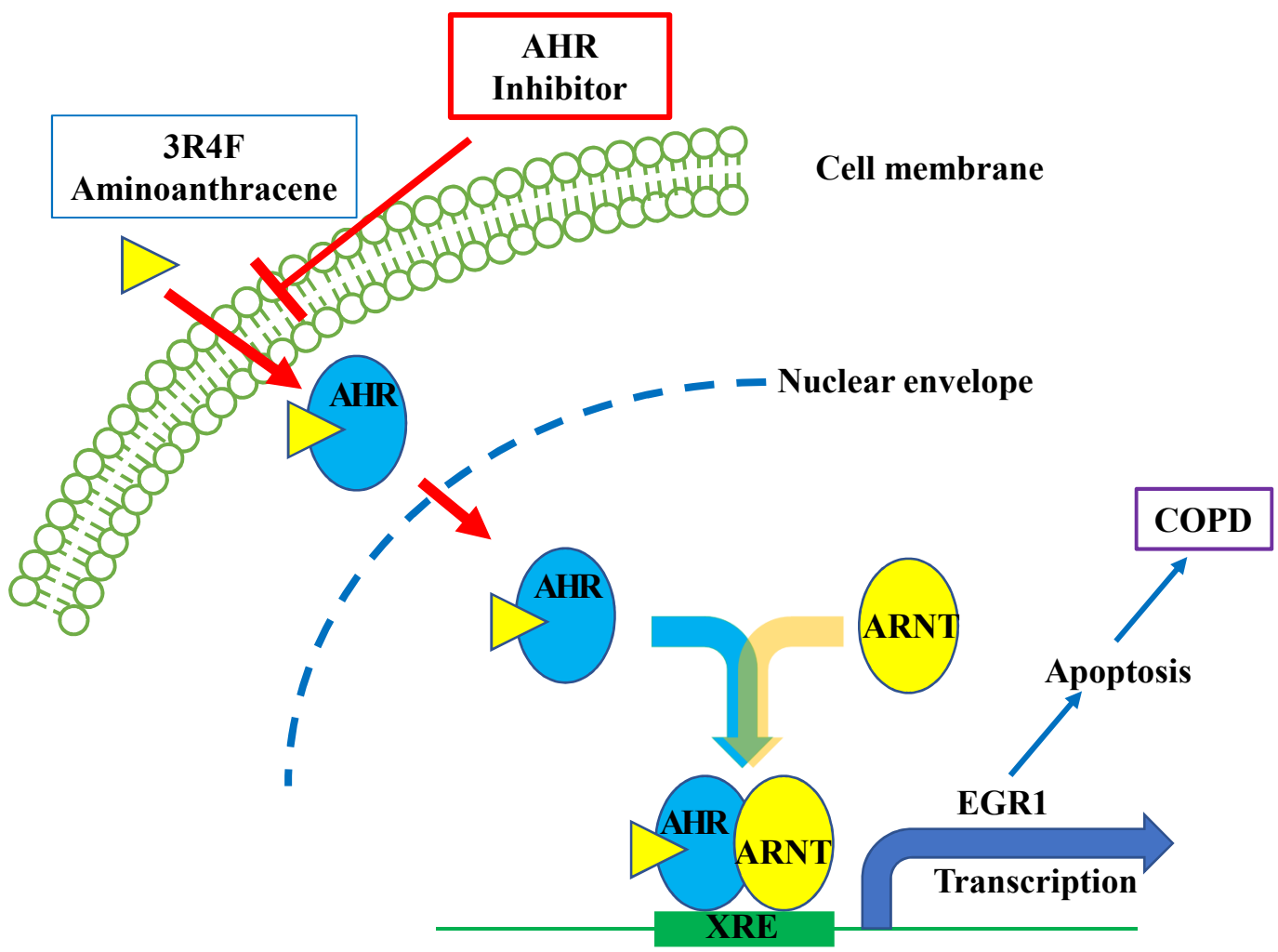
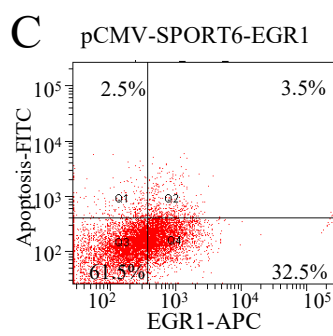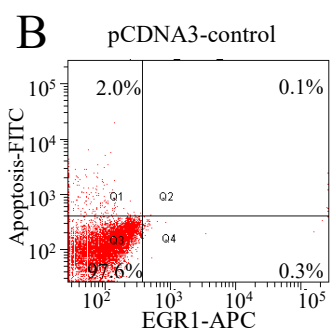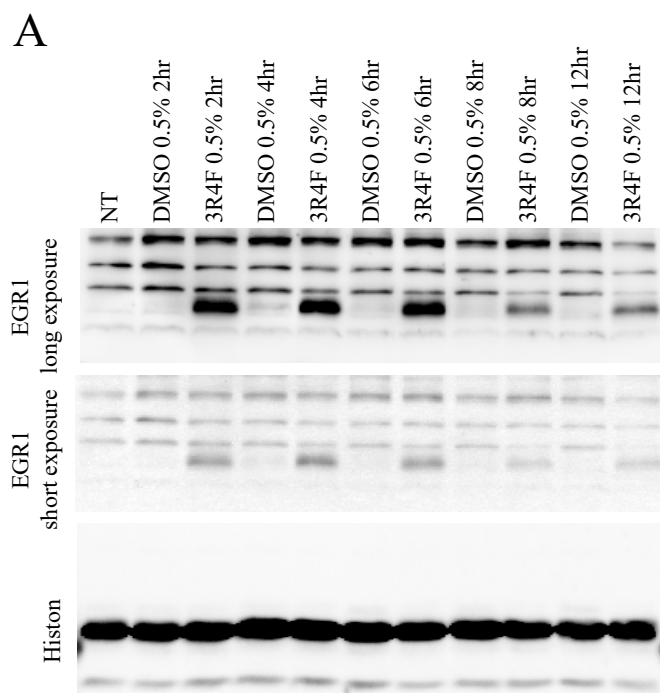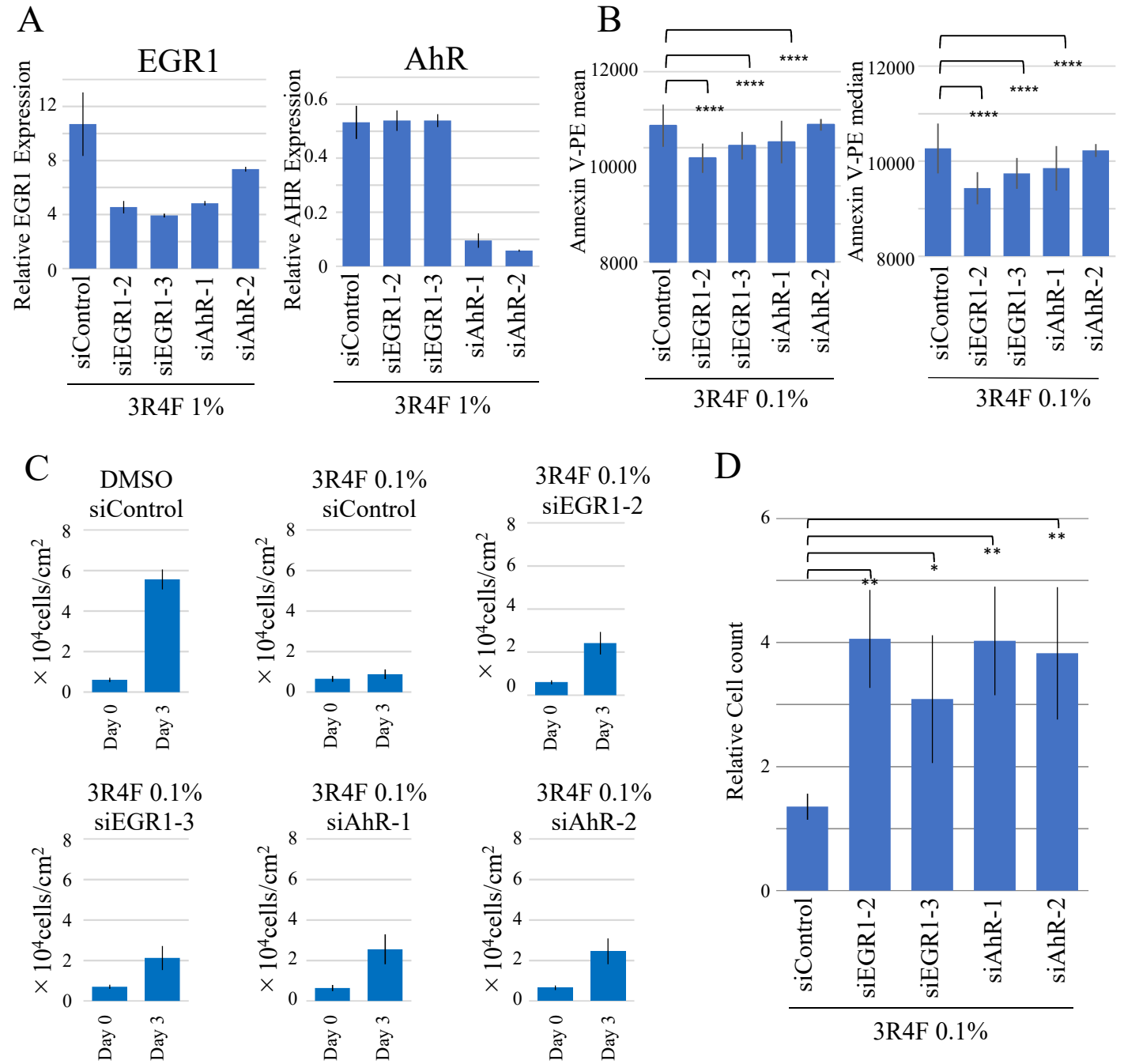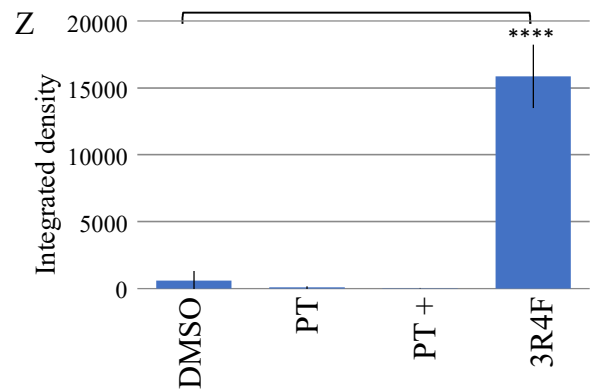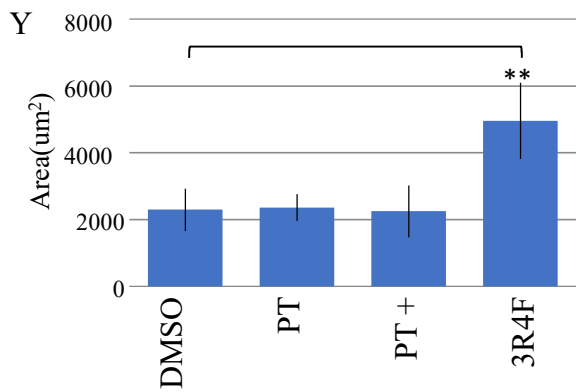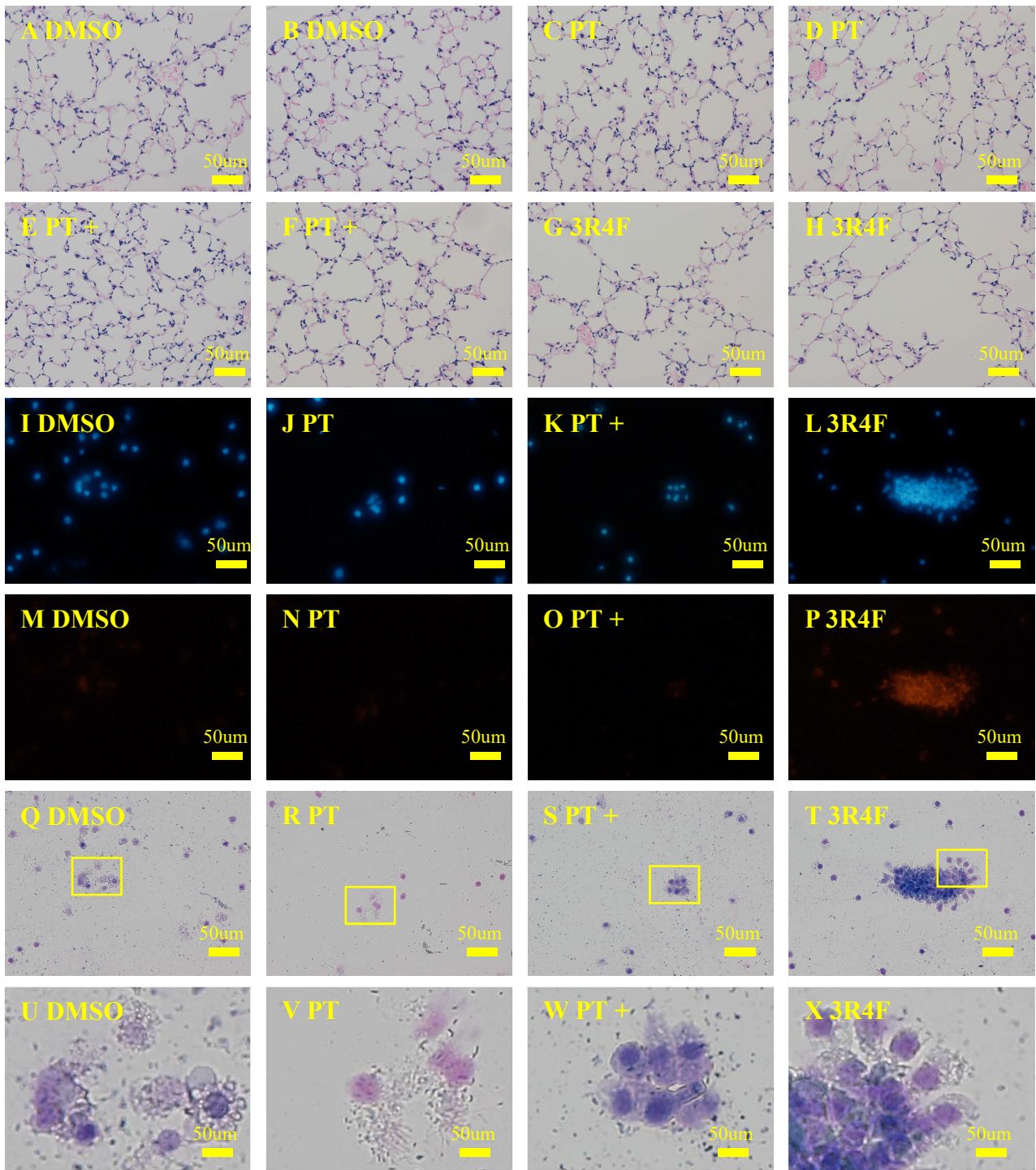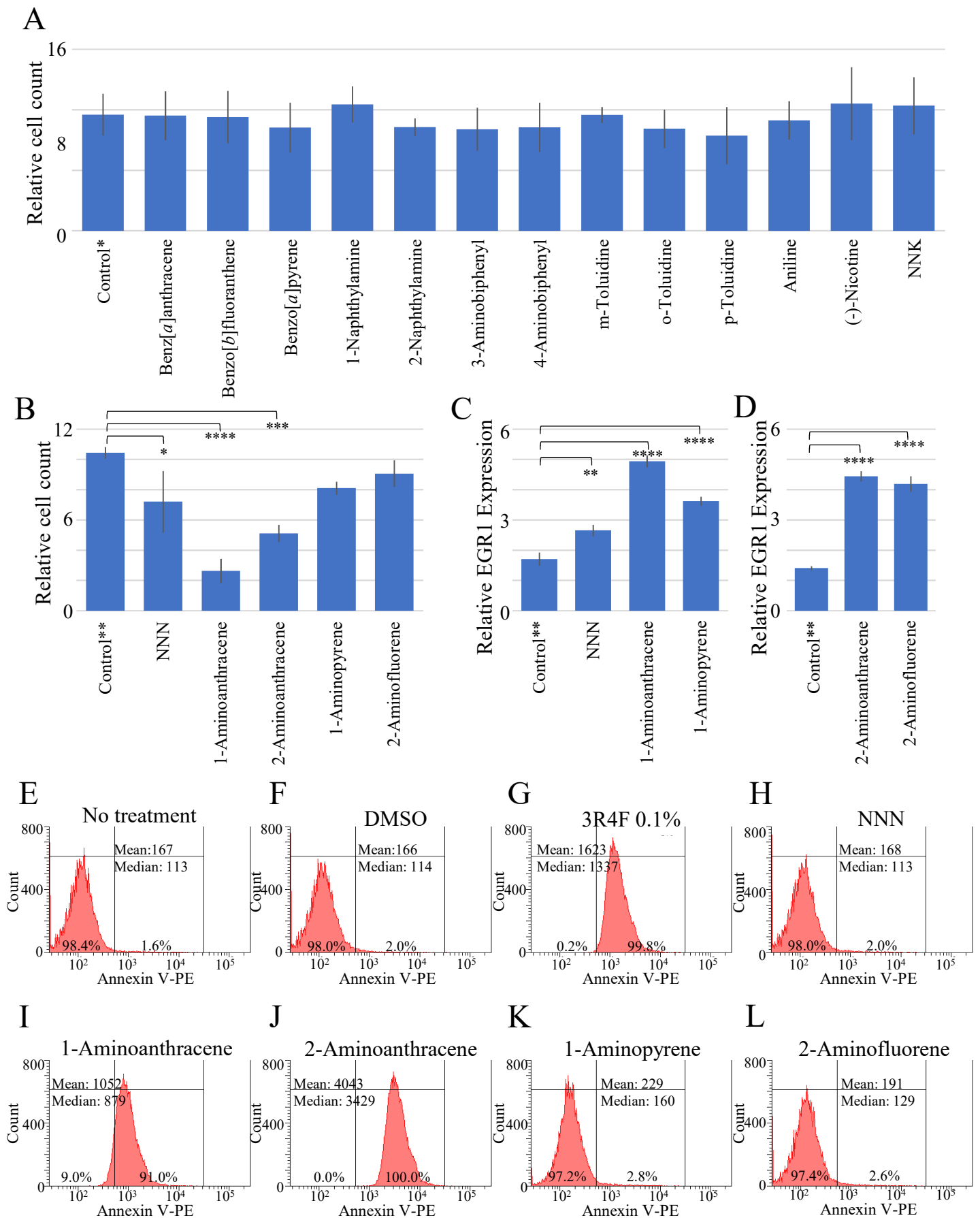Figure 1 Hattori et al

Figure 2 Hattori et al

A

EGR1 long exposure

NT | DMSO 0.5% 2hr | 3R4F 0.5% 2hr | DMSO 0.5% 4hr | 3R4F 0.5% 4hr | DMSO 0.5% 6hr | 3R4F 0.5% 6hr | DMSO 0.5% 8hr | 3R4F 0.5% 8hr | DMSO 0.5% 12hr | 3R4F 0.5% 12hr

EGR1 short exposure

Histon

B pCDNA3-control

Apoptosis-FITC

10^5 2.0%   0.1%
10^4
10^3 Q2
        Q1
10^2 Q4
       97.6%   0.3%
    10^2 10^3 10^4 10^5
         EGR1-APC

C pCMV-SPORT6-EGR1

Apoptosis-FITC

10^5 2.5%   3.5%
10^4
10^3 Q1   Q2
10^2
       61.5%   32.5%
    10^2 10^3 10^4 10^5
         EGR1-APC
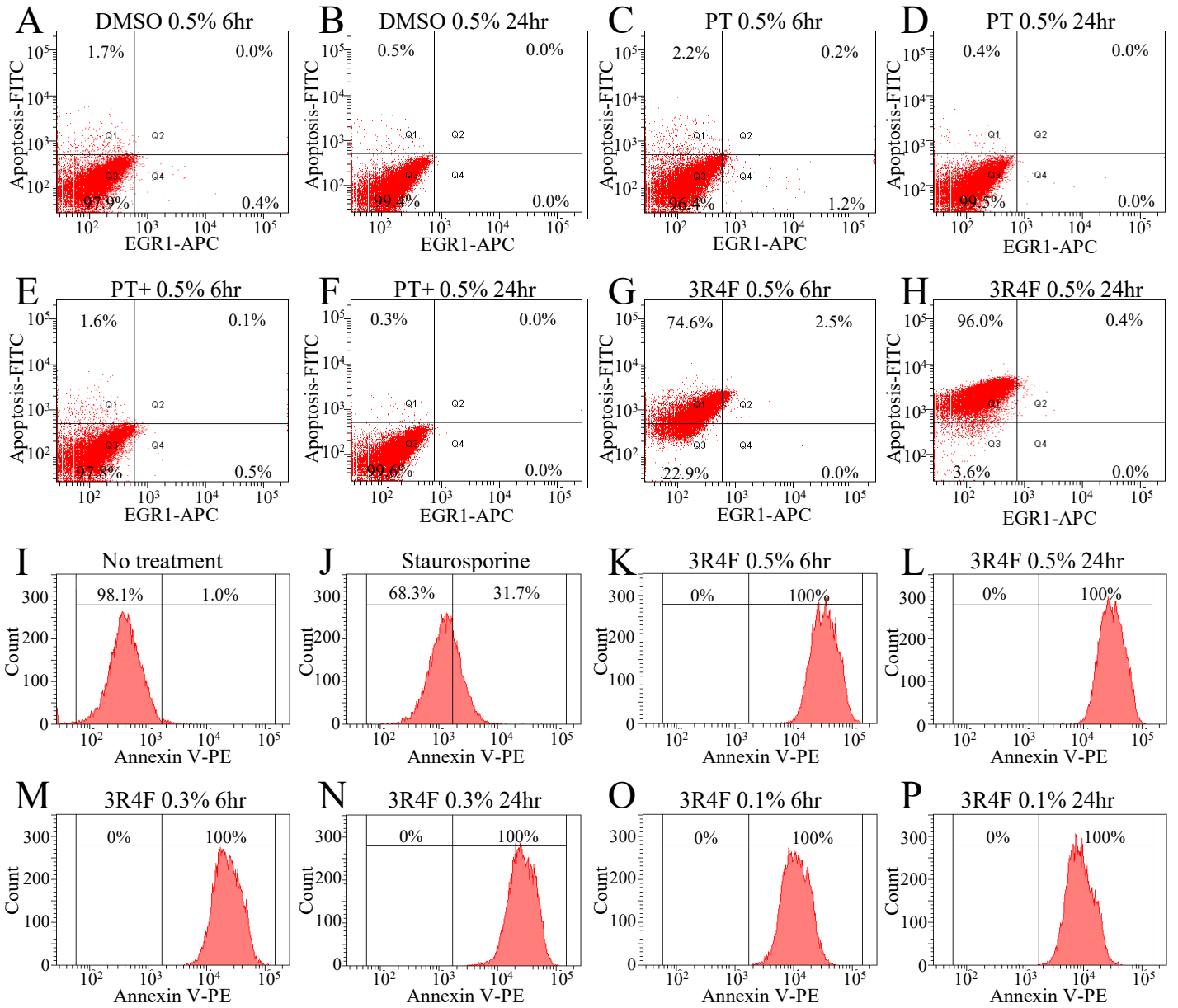
Figure 3 Hattori et al

Figure 4 Hattori et al
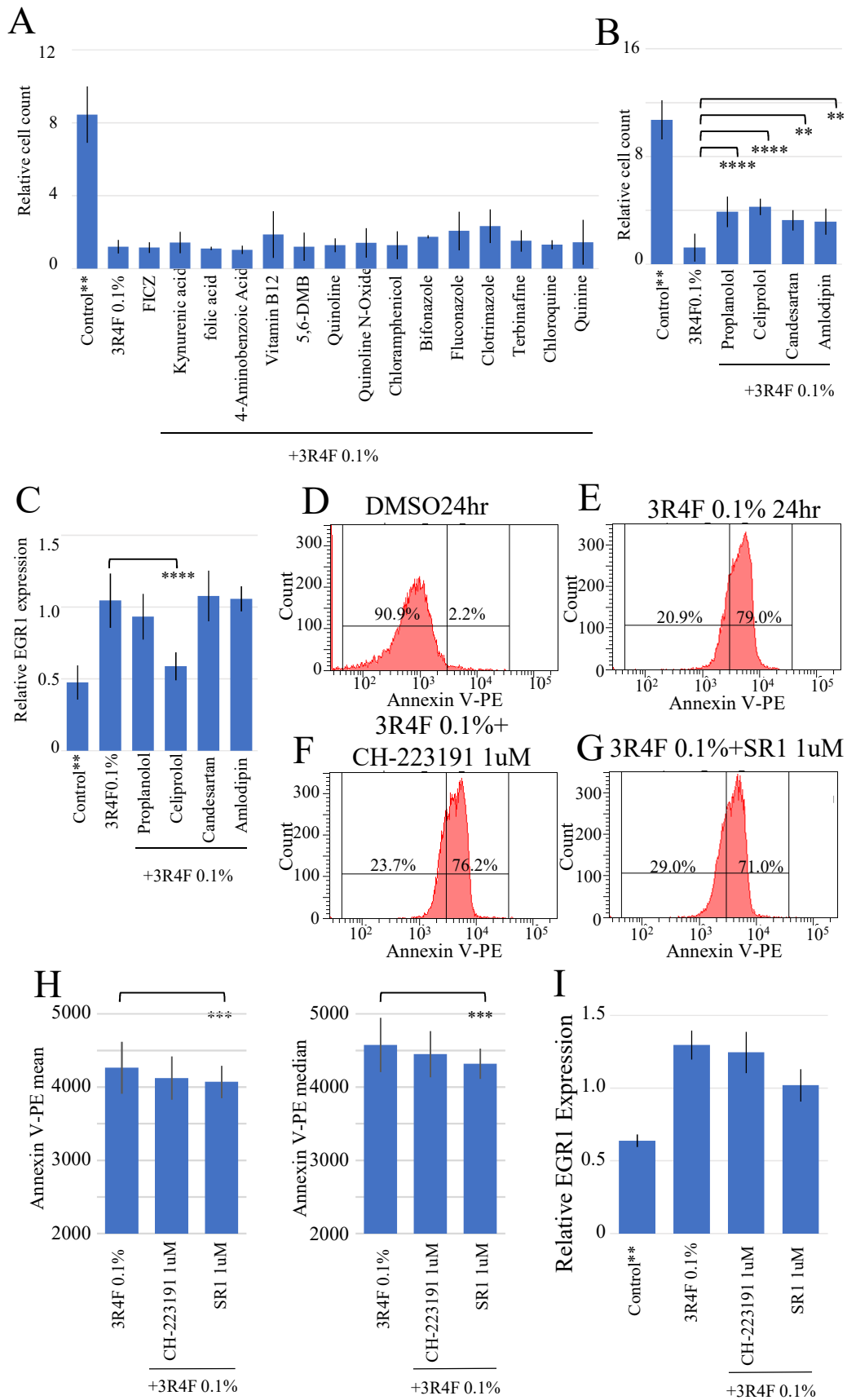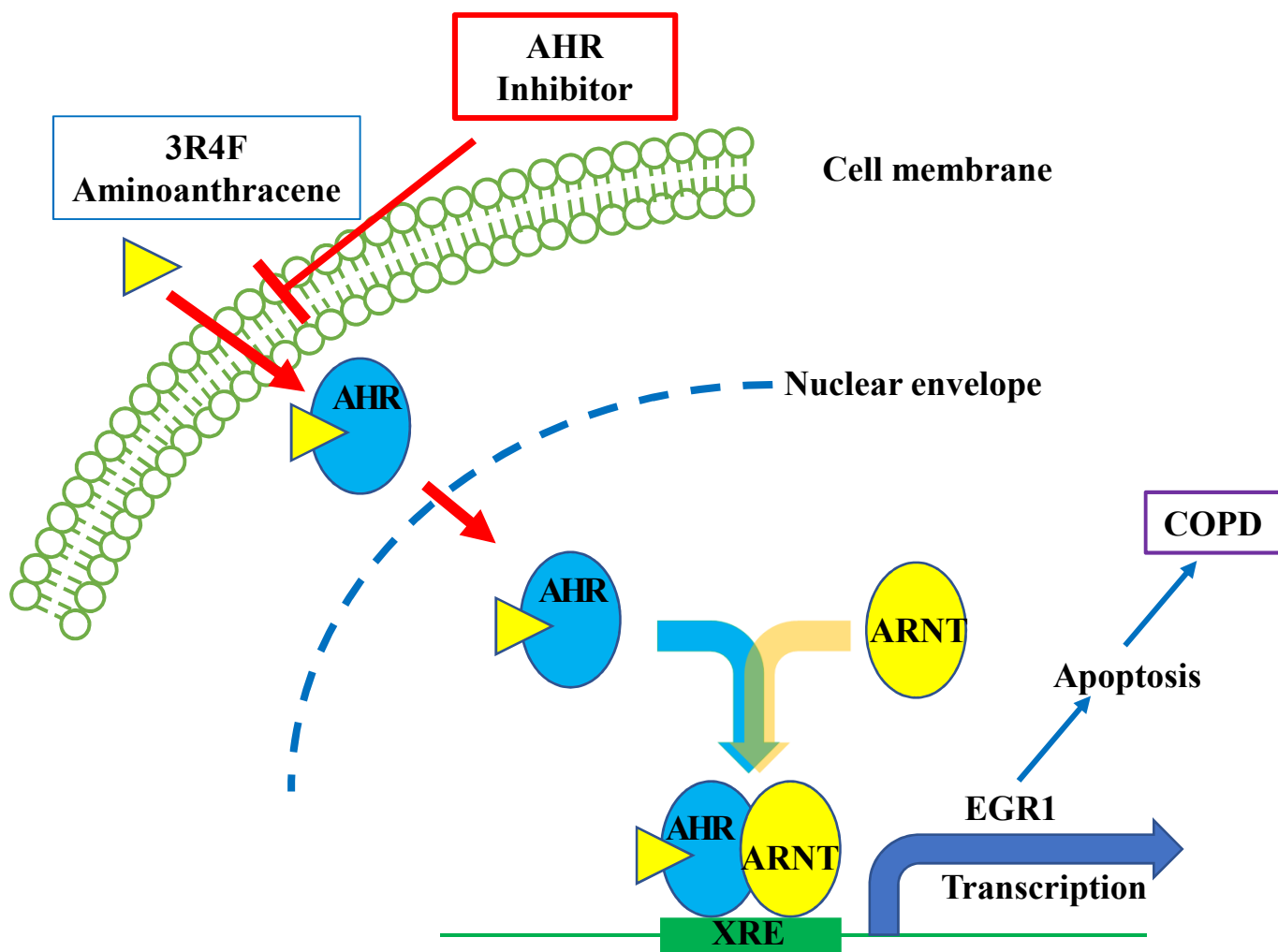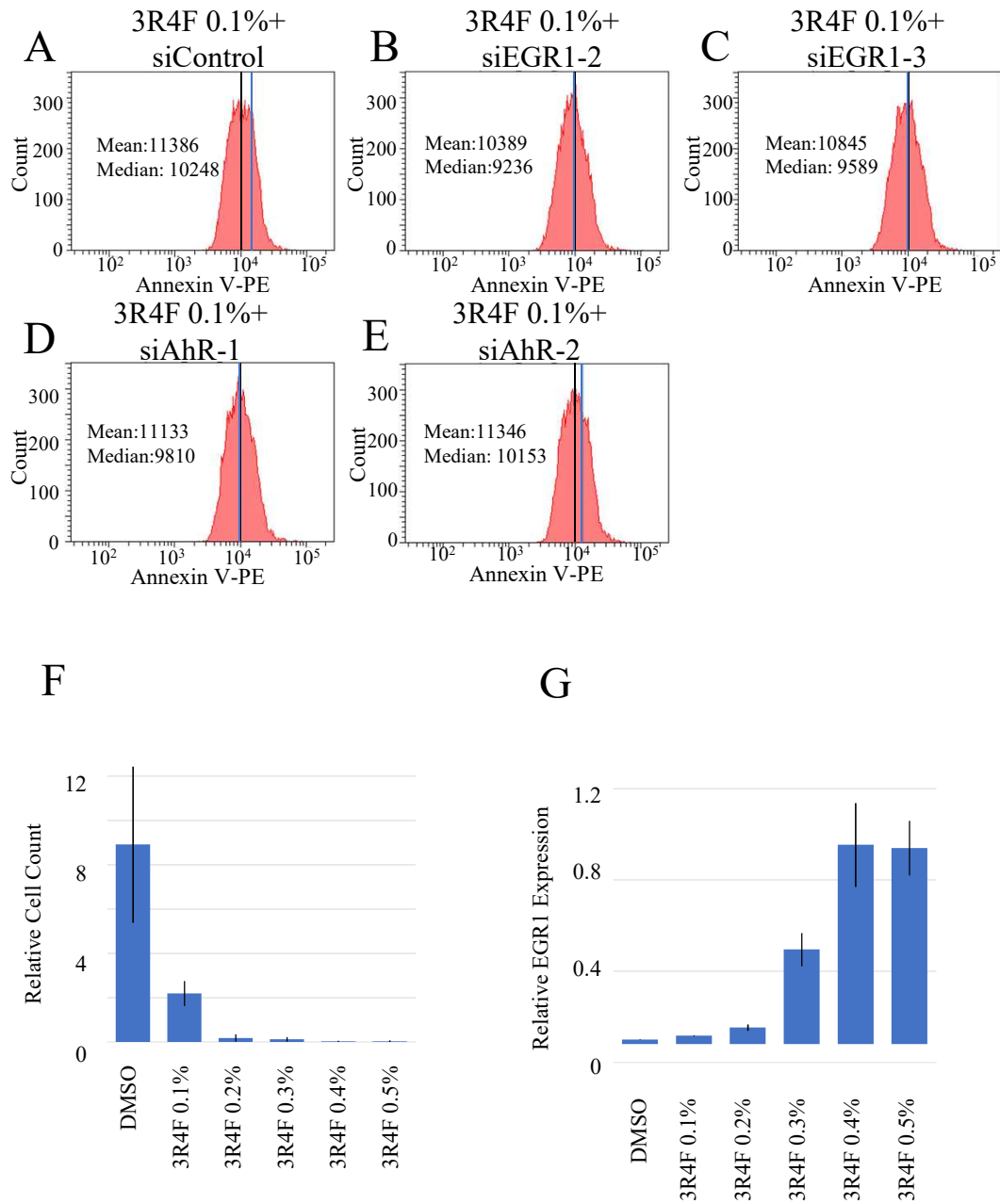
Figure 5 Hattori et al
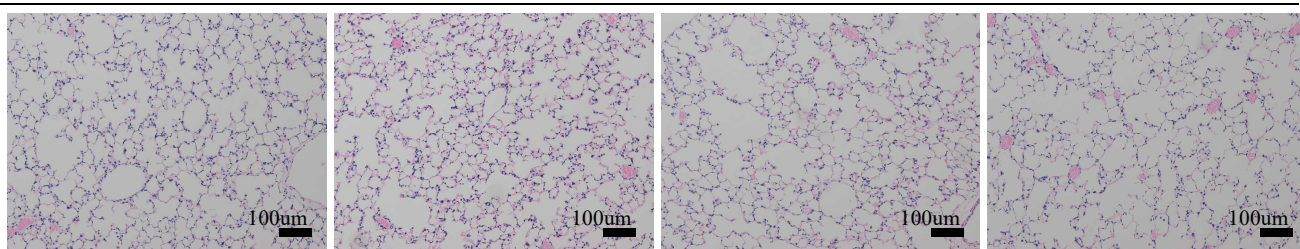
Figure 6 Hattori et al

Figure 7

Supplementary figure 1 Hattori et al

A 3R4F 0.1%+ siControl
Mean:11386
Median: 10248

B 3R4F 0.1%+ siEGR1-2
Mean:10389
Median:9236

C 3R4F 0.1%+ siEGR1-3
Mean:10845
Median: 9589

D 3R4F 0.1%+ siAhR-1
Mean:11133
Median:9810

E 3R4F 0.1%+ siAhR-2
Mean:11346
Median: 10153

F

G

Supplementary figure 2 Hattori et al

A DMSO
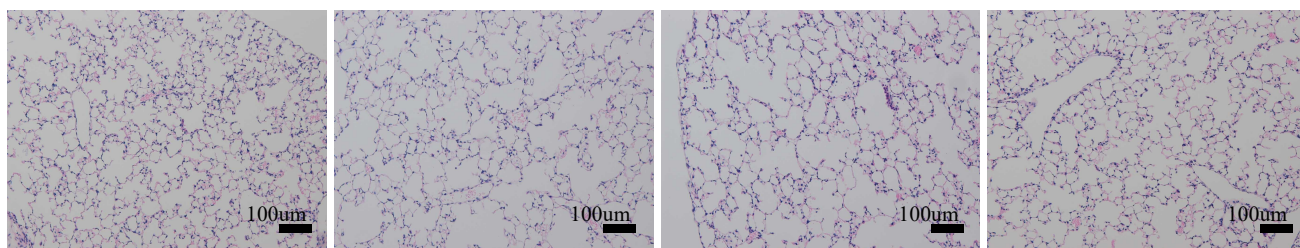
B PT

C PT +
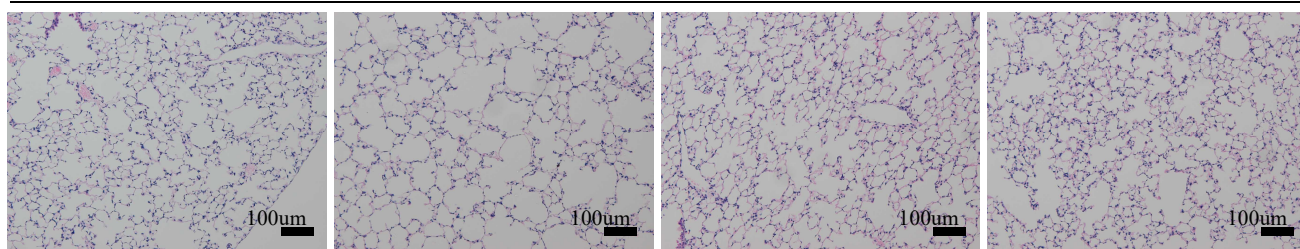
D 3R4F
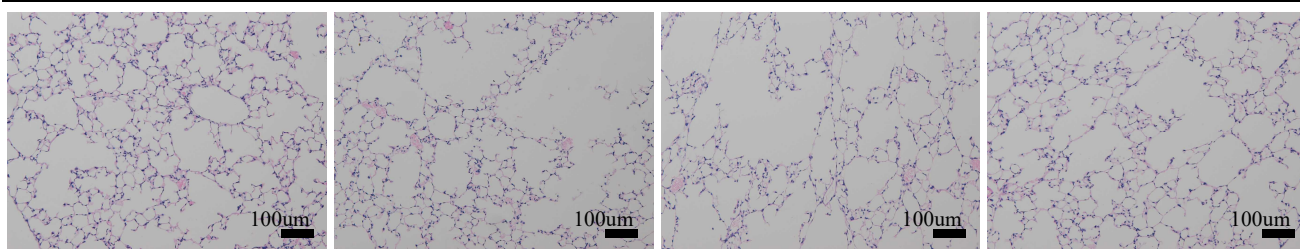
A DMSO 50um	B PT 50um	C PT + 50um	D 3R4F 50um
E DMSO 50um	F PT 50um	G PT + 50um	H3R4F 50um
I DMSO 50um	J PT 50um	K PT + 50um	L 3R4F 50um
M DMSO 50um	N PT 50um	O PT + 50um	P 3R4F 50um
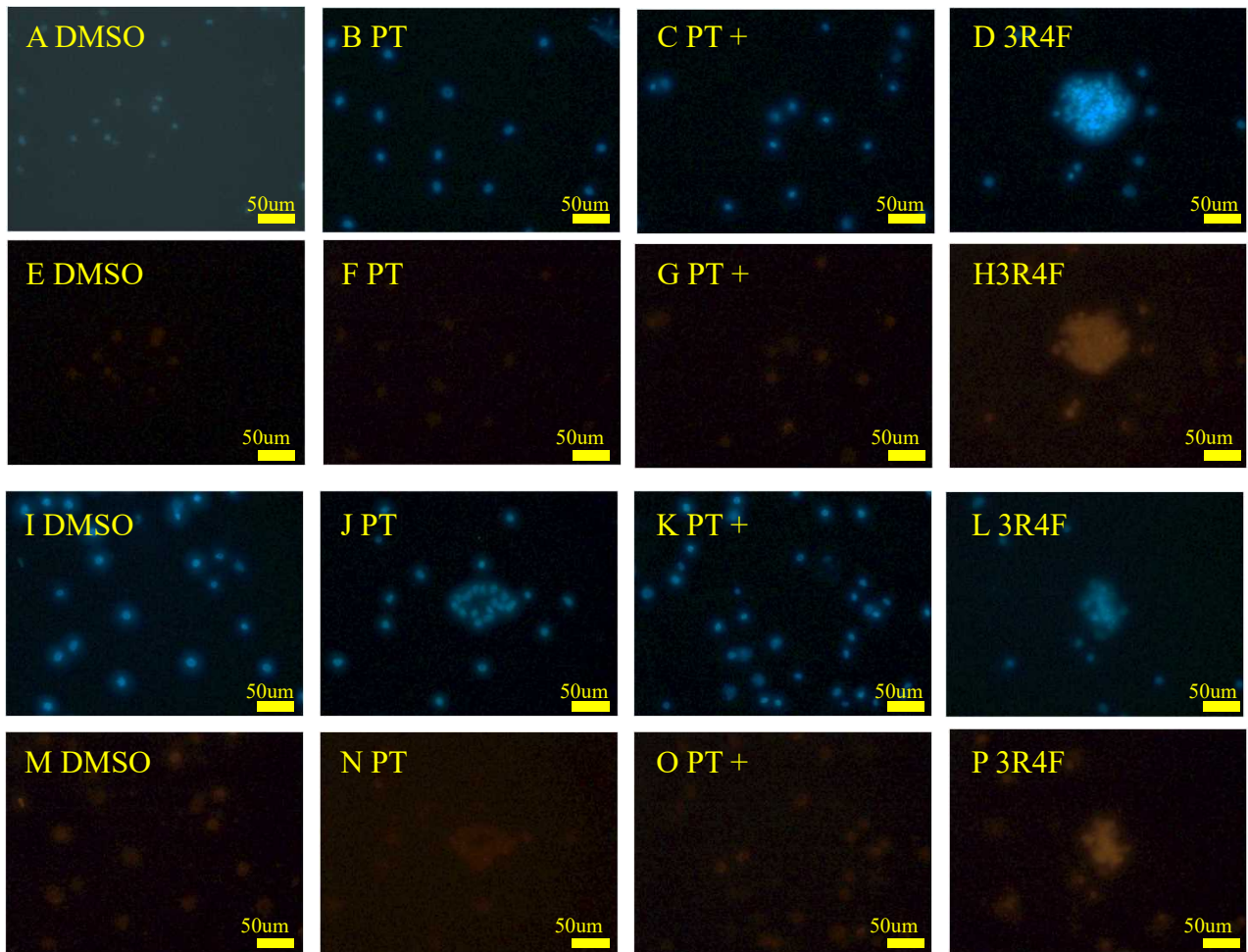
Table 1. Chemical compounds used in experiments summarized in Figure 4.

	Chemical compound	solvent
1	Benz[*a*]anthracene standard	Acetone
2	Benzo[*b*]fluoranthene	Acetone
3	Benzo[*a*]pyrene standard	Acetone
4	1-Naphthylamine	Methanol
5	2-Naphthylamine	acetonitrile
6	3-Aminobiphenyl	Methanol
7	4-Aminobiphenyl	Methanol
8	m-Toluidine	Methanol
9	o-Toluidine	Methanol
10	p-Toluidine	Methanol
11	Aniline	Methanol
12	(-)-Nicotine solution	Methanol
13	*N* -Nitrosonornicotine	DMSO
14	4-(methylnitrosamino)- 1-(3-pyridyl)-1-butanone	Methanol
15	Pentobarbital	Methanol
16	4-Nitroquinoline-1-oxide	DMSO
17	1-Aminoanthracene	DMSO
18	2-Aminoanthracene	DMSO
19	1-Aminopyrene	DMSO
20	2-Aminofluorene	DMSO

Table 2. Drugs used in the experiments summarized in Figure 5.

	drug	solvent
1	6-Formylindolo[3,2-b]carbazole	DMSO
2	Kynurenic acid	DMSO
3	Folic acid	DMSO
4	4-Aminobenzoic acid	DMSO
5	Vitamin B12	Water
6	5, 6-Dimethylbenzimidazole	DMSO
7	Quinoline	Methanol
8	Quinoline N-Oxide	DMSO
9	Chloramphenicol	DMSO
10	Bifonazole	DMSO
11	Fluconazole	DMSO
12	Clotrimazole	DMSO
13	Terbinafine	DMSO
14	Chloroquine Diphosphate	Water
15	(-)-Quinine Sulfate Dihydrate	Methanol
16	Proplanolol Hydrochloride	DMSO
17	Celiprolol Hydrochloride	DMSO
18	Candesartan	DMSO
19	Amlodipine	DMSO